ISSN 0915-6364

NATIONAL INSTITUTE FOR FUSION SCIENCE

Cross Sections for Electron-induced Resonant Vibrational Excitations in Polyatomic Molecules

H. Kato, M. Hoshino, H. Kawahara, C. Makochekanwa, S.J. Buckman, M.J. Brunger, H. Cho, M. Kimura, D. Kato, H.A. Sakaue, I. Murakami, T. Kato and H. Tanaka

(Received - Dec. 12, 2008)

NIFS-DATA-105 Mar. 3, 2009

RESEARCH REPORT
NIFS-DATA Series

TOKI, JAPAN

Cross Sections for Electron-induced Resonant Vibrational Excitations in Polyatomic Molecules

H. Kato[1], M. Hoshino[1], H. Kawahara[1], C. Makochekanwa[1,2], S. J. Buckman[2], M. J. Brunger[3], H. Cho[4], M. Kimura[5], D. Kato[6], H. A. Sakaue[6], I. Murakami[6], T. Kato[6] and H. Tanaka[1]

[1]Department of Physics, Sophia University, Tokyo 102-8554, Japan
[2]Centre for Antimatter-Matter Studies, Australian National University, Canberra ACT 0200, Australia
[3]Centre for Antimatter-Matter Studies, Flinders University, Adelaide SA 5001, Australia
[4]Department of Physics, Chungnam National University, Daejeon 305-764, Korea
[5]Graduate School of Sciences, Kyushu University, Fukuoka 812-8581, Japan
[6]National Institute of Fusion Science, Toki 590-5292, Japan

1. Introduction
2. Experimental Techniques for Precision Measurements of Electron Energy Loss Spectra and Vibrational Excitation Functions
3. Benchmark Data for Vibrational Excitation
   A. Fusion Plasma – Related Gases
   B. Processing Plasma – Related Gases
   C. Environmental Issues – Related Gases
4. Concluding Remarks

This work was supported in part by the IAEA, CUP, MEXT and the ARC.

Abstract

We continue our review of experimental data for electron-polyatomic molecule collisions in connection with fusion and processing plasmas, as well as with the associated environmental issues. In this case we focus on vibrational excitation processes, in particular what vibrational modes can be identified in electron energy loss experiments and which of these modes are resonantly enhanced due to the temporary capture of the incident electron by the species in question. In this latter respect we report indicative excitation function data, all of which were originally measured at Sophia University and for which the differential cross section, for excitation of the relevant mode, are studied as a function of the incident electron energy at a fixed scattered electron angle. Unlike our previous compilation (NIFS–DATA–101) for elastic scattering, which was conducted over a broad range of energies (1–100 eV), vibrational excitation cross sections usually only become significant when the resonance enhancement process occurs. As a consequence, this survey encompasses incident electron energies between 1–30 eV. Consistent with our first report, no detailed comparison is made here with any other data that might be available in the literature. This course of action was once again adopted in order to keep this report to a sensible length.

Keywords
electron-molecule collisions, vibrational excitation processes, excitation functions, resonant electron scattering

1. Introduction

In Hoshino et al. (2008) we described why the interaction of electrons with atoms and molecules is an essential process in many areas of modern science and technology, including nanotechnology. We therefore do not repeat that detail here, rather we consider the importance of resonances. A resonance can be thought of as a temporary bound state of an electron with a molecule, that is formed by an effective-potential well. This well might, for instance, be due to the combination of the (repulsive) centrifugal force for a definite orbital angular momentum and an (attractive) molecular potential. The temporary bound state may be viewed as an excited state of a negative ion, that is, the system of the neutral molecule plus the electron, which may or may not be bound in the ground state. If the temporary bound state is sufficiently stable against auto-detachment, and has a lifetime much longer than the period of a molecular vibration, then the nuclei will experience forces that are different from those in the original molecule. This causes conversion of a part of the electron's energy to the nuclear vibrational degrees of freedom. This mechanism of vibrational excitation can be more efficient than a direct transfer of the electron's energy to nuclear motion, which can occur at any electron energy above the relevant vibrational threshold but is, in general, much less efficient because of the large ratio of the nuclear mass to the electron mass. Note that resonances are also an important mechanism for dissociative electron attachment (Pelc et al. 2002) resulting in the formation of stable negative-ion fragments. While such a process is clearly very important in its own right, in this report we concentrate on the effects of resonances on various vibrational modes in polyatomic molecules. Furthermore, as noted briefly above and by Schulz in his seminal articles (Schulz 1973a,b, Allan), "resonances occurring in electron impact often enhance inelastic cross sections by orders of magnitude" over the non-resonant scattering case. As a consequence, the vibrational excitation data we report here focuses on an incident electron energy range where experience dictates that resonance effects predominate. Namely, we look at incident electron energies in the range ~1–30 eV.

Three broad classes of polyatomic molecular targets have been considered in this report (see Table 1), and sorted according to whether they are fusion plasma-related gases, processing plasma-related gases or environmentally-related gases. In each case we provide details of the vibrational modes that might be expected to be excited by electron impact, and then a corresponding electron energy-loss spectrum (EELS) to see which of these modes can be resolved in practice in our experimental apparatus. In addition, representative vibrational excitation functions, again for each molecule, for the most important modes, are presented. These excitation functions provide graphic evidence for any resonance enhancement in the scattering process. While it is true that such excitation functions are not the cross sections (integral cross section: ICS) needed for the modelling of atmospheric and technological phenomena, to a first order they can be used to generate such data. Specifically, by assuming the scattering process is isotropic the excitation functions presented in this report simply need to be multiplied by 4π to generate the ICSs used for modelling studies. There is no doubt that in many cases the assumption of isotropic scattering is simplistic, nonetheless it does allow estimates for the relevant integral cross sections to be obtained when in many cases they would not otherwise be available.

Finally, we note that as Hoshino et al. (2008) previously defined what we mean by a cross section and the different types of cross sections that might be measured or calculated, we do not provide this description again here. Similarly the instrumentation needed to make such measurements was also discussed in our first report, to whom the interested reader is referred for those details.

References:

M. Hoshino, H. Kato, C. Makochekanwa, S. J. Buckman, M. J. Brunger, H. Cho, M. Kimura, D. Kato, I. Murakami, T. Kato and H. Tanaka, NIFS–DATA–101: "Elastic Differential Cross Sections for Electron Collisions with Polyatomic Molecules" (National Institute for Fusion Science, Toki, Japan, 2008), ISSN 0915-6364, pages 1–60.

A. Pelc, W. Sailer, P. Scheier, M. Probst, N. J. Mason, E. Illenberger and T. D. Märk, *Chem. Phys. Letts*. 361 (2002), 277.
G. J. Schulz*, Rev. Mod. Phys*. 45 (1973a), 378.
G. J. Schulz, *Rev. Mod. Phys.* 45 (1973b), 423.
M. Allan, *J. Electron Spectrosc. Relat. Phenom.* 48 (1989), 219

2. Experimental Techniques for Precision Measurements of Electron Energy Loss Spectra and Vibrational Excitation Functions

In our original NIFS-DATA-101 report we described how absolute elastic differential cross sections for polyatomic molecules could be measured using the relative flow technique (Srivastava et al. 1975), with absolute elastic differential cross sections for helium gas (Boesten and Tanaka 1992) employed as the reference standard. In this report the measurement of energy loss spectra and vibrational excitation functions present slightly different challenges, so that some brief further details are required.

In the measurement of the energy loss spectra, the incident electron energy is fixed and the number of scattered electrons is recorded as a function of the energy loss (i.e. the energy that the incident electrons give up to the target molecules) for a given scattered electron angle. These spectra are very useful, as they serve to identify the elastic and various vibrational modes excited in the collisional process. The important aspect in these measurements is to ensure that the transmission of the scattered electrons detected in the energy analyser, which come out with varying scattered energies depending on the process involved, is constant for the energy loss range of interest. At Sophia University detailed electron optics simulations suggested that for the incident energy range of interest (1–30 eV) and for energy loss (ΔE) processes in the range 0 eV $\leq \Delta E \leq$ 0.5 eV, this criterion is met.

Using the energy loss spectra, the particular vibrational feature of interest can be selected. In practice this means that the energy loss value (ΔE) of that feature is fixed at the appropriate value. The excitation function for that feature, again at a fixed scattered electron angle, is now measured by recording the number of inelastically scattered electrons (at ΔE) as a function of the incident electron beam energy. Here the challenge is to keep the focal properties and incident electron beam current as constant as possible over the 1–30 eV range, or alternatively to calibrate the spectrometer performance against a known result. In this respect the shapes of the known excitation functions for helium elastic scattering (over a vast range of scattering angles) provide a convenient calibration tool. Finally, the excitation function needs to be placed on an absolute scale, with a minor variant of the relative flow technique, again using helium as the standard, serving this purpose.

The absolute incident electron energy scale is calibrated by observing either the position of the second resonance peak in the N_2 $\nu' = 0$–1 excitation function at 60° (E = 2.198 eV, Rohr 1977), or the position of the $He^-1s2s^2\ ^2S$ resonance at 19.367 eV (Brunt et al 1977) in the elastic channel. Typical experimental errors in the vibrational excitation function measurements are better than 30%. They arise from a combination, in quadrature, of the statistical uncertainties on the scattered electron count rates together with those arising from measurements of parameters such as the electron current, gas pressure, the analyser transmission and normalisation technique. The latter also includes an uncertainty on the helium cross sections.

References:

L. Boesten and H. Tanaka, *At. Data. Nucl. Data Tables* 52, 25 (1992).
S. K. Srivastava, A. Chutjian and S. Trajmar, *J. Chem. Phys*. 63, 2659 (1975).
K. Rohr, *J. Phys*. *B*: *At. Mol. Phys.* 10, 2215 (1977).
J. N. H. Brunt, G. C. King and F. H. Read*, J. Phys. B*: *At. Mol. Phys.* 10, 1289 (1977).

3. Benchmark Data for Vibrational Excitation

In Table 1 below we summarise the broad classes of polyatomic molecules, and specific molecules within these classes, that we will consider in this report.

Table 1: List of molecules considered in this report

A. Fusion Plasma-related Gases

CH_4, C_2H_6, C_3H_8, C_3H_6, cyclo-C_3H_6, isomers-C_3H_4

B. Processing Plasma-related Gases

C_2F_4, C_2F_6, C_3F_8, cyclo-C_4F_8, C_2F_4, C_6F_6, C_3F_6
CH_3F, CH_2F_2, CHF_3
NF_3
SiH_4, Si_2H_6, GeH_4, SiF_4
F_2CO

C. Environmental Issues-related Gases

CF_3Cl, CF_3Br, CF_3I
CO_2, N_2O, CO, OCS, CS_2
H_2O, H_2CO
$(CH_3)_2O$, $(CH_3)_2CO$
C_6H_6, $C_6H_5CH_3$, $C_6H_5CF_3$
1,1-$C_2H_2F_2$

We now consider each of these sequentially and present the relevant data.

A. Fusion Plasma-Related Gases

A1. $\underline{CH_4}$

Table A1.1. Vibrational fundamental modes.

Vibrational mode	Energy (eV)	Species
ν_1 (Sym str)	0.362	a_1
ν_2 (Deg deform)	0.190	e
ν_3 (Deg str)	0.374	f_2
ν_4 (Deg deform)	0.162	f_2

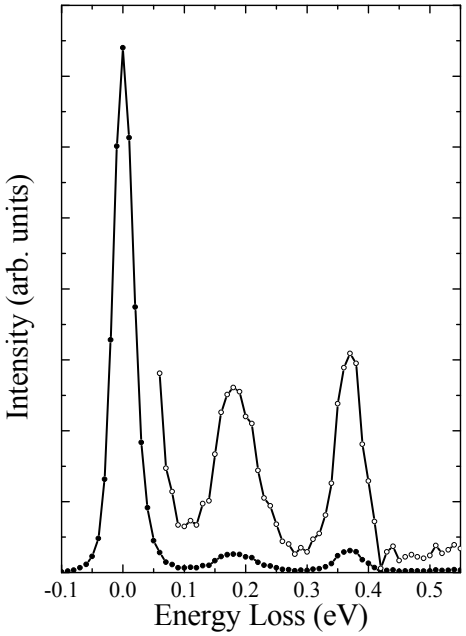

Figure A1.1. Energy loss spectrum of CH_4 at impact energy 7 eV for a scattering angle of 90 degrees.

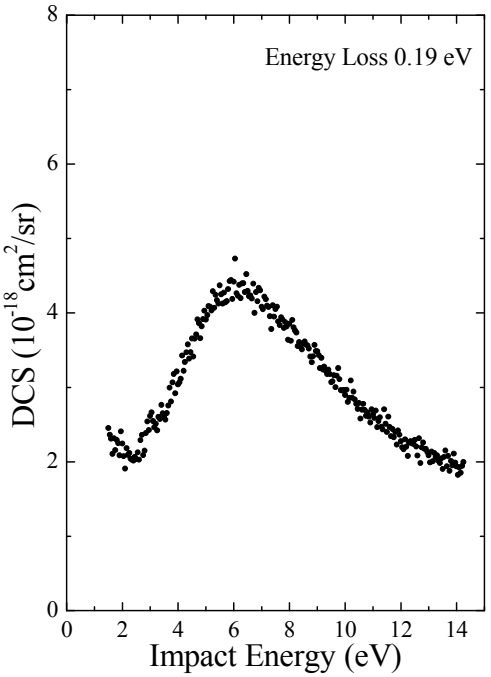

Figure A1.2. Vibrational excitation function of CH_4 at the scattering angle of 90 degrees.

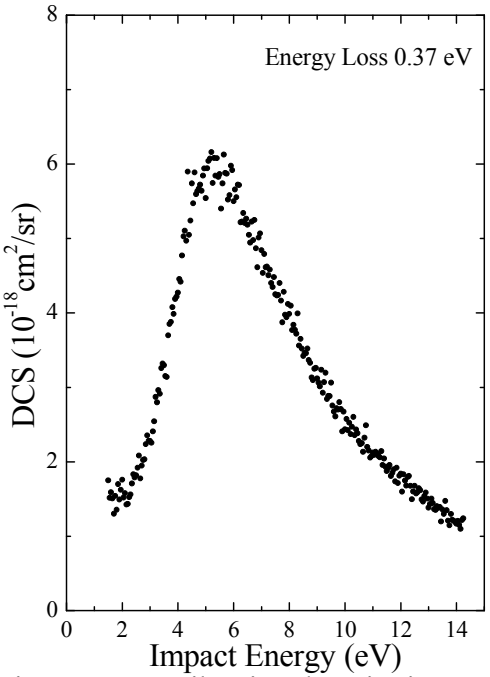

Figure A1.3. Vibrational excitation function of CH_4 at the scattering angle of 90 degrees.

A2. C_2H_6

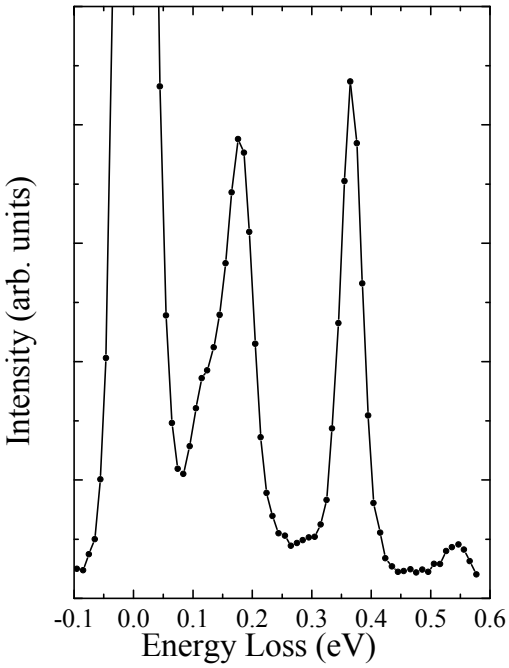

Figure A2.1. Energy loss spectrum of C_2H_6 at impact energy 7.5 eV for a scattering angle 90 degrees.

Table A2.1. Vibrational fundamental modes.

Vibrational mode	Energy (eV)	Species
ν_1 (CH_3 s-str)	0.366	a_{1g}
ν_2 (CH_3 s-deform)	0.172	a_{1g}
ν_3 (CC str)	0.123	a_{1g}
ν_4 (Torsion)	0.036	a_{1u}
ν_5 (CH_3 s-str)	0.359	a_{2u}
ν_6 (CH_3 s-deform)	0.171	a_{2u}
ν_7 (CH_3 d-str)	0.368	e_g
ν_8 (CH_3 d-deform)	0.182	e_g
ν_9 (CH_3 rock)	0.148	e_g
ν_{10} (CH_3 d-str)	0.370	e_u
ν_{11} (CH_3 d-deform)	0.182	e_u
ν_{12} (CH_3 rock)	0.102	e_u

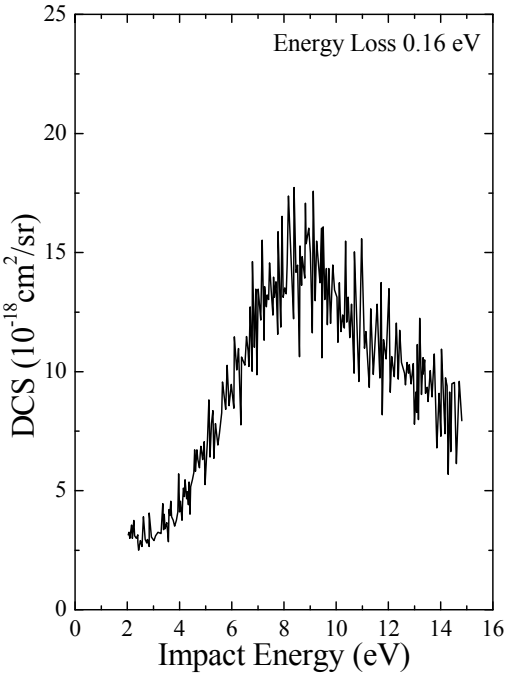

Figure A2.2. Vibrational excitation function of C_2H_6 at the scattering angle of 90 degrees.

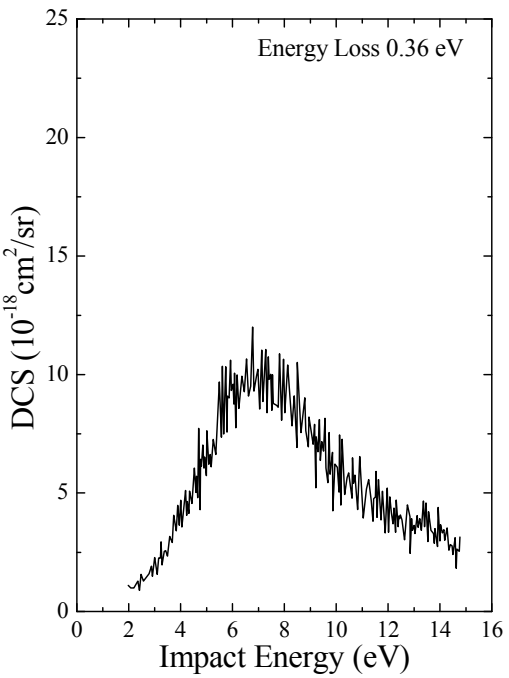

Figure A2.3. Vibrational excitation function of C_2H_6 at the scattering angle of 90 degrees.

Reference:

L. Boesten, H. Tanaka, M. Kubo, H. Sato, M. Kimura, M. A. Dillon and D. Spence, *J. Phys. B* **23**, 1905 (1990).

A3. C_3H_8

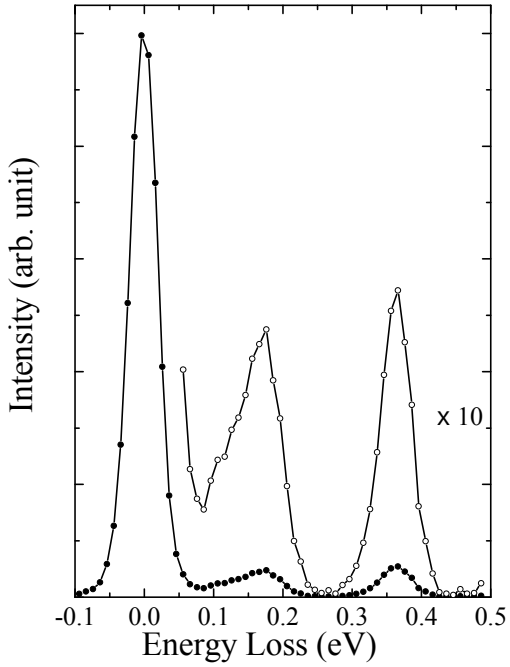

Figure A3.1. Energy loss spectrum of C_3H_8 at impact energy 7.5 eV for a scattering angle 70 degrees.

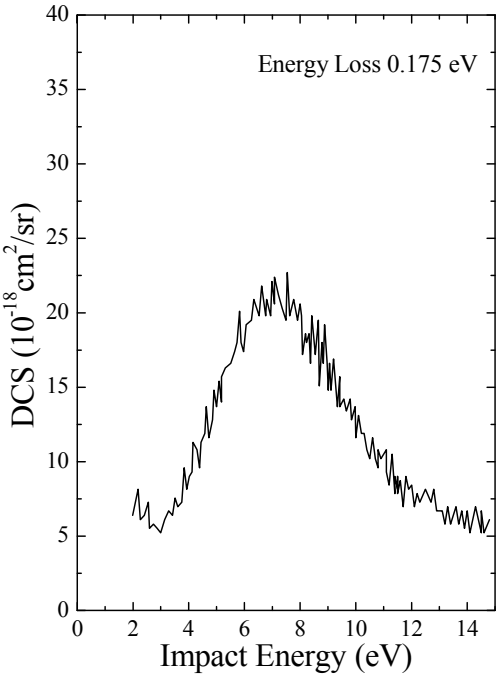

Figure A3.2. Vibrational excitation function of C_3H_8 at the scattering angle of 90 degrees.

Table A3.1. Vibrational fundamental modes

Vibrational mode	Energy (eV)	Species
ν_1 (CH_3 d-str)	0.369	a_1
ν_2 (CH_3 s-str)	0.367	a_1
ν_3 (CH_2 s-str)	0.358	a_1
ν_4 (CH_3 d-deform)	0.183	a_1
ν_5 (CH_2 scis)	0.181	a_1
ν_6 (CH_3 s-deform)	0.173	a_1
ν_7 (CH_3 rock)	0.144	a_1
ν_8 (CC str)	0.108	a_1
ν_9 (CCC deform)	0.046	a_1
ν_{10} (CH_3 d-str)	0.368	a_2
ν_{11} (CH_3 d-deform)	0.180	a_2
ν_{12} (CH_2 twist)	0.158	a_2
ν_{13} (CH_3 rock)	0.117	a_2
ν_{14} (Torsion)	0.027	a_2
ν_{15} (CH_3 d-str)	0.368	b_1
ν_{16} (CH_3 s-str)	0.358	b_1
ν_{17} (CH_3 d-deform)	0.182	b_1
ν_{18} (CH_3 s-deform)	0.171	b_1
ν_{19} (CH_2 wag)	0.166	b_1
ν_{20} (CC str)	0.131	b_1
ν_{21} (CH_3 rock)	0.114	b_1
ν_{22} (CH_3 d-str)	0.369	b_2
ν_{23} (CH_2 a-str)	0.368	b_2
ν_{24} (CH_3 d-deform)	0.183	b_2
ν_{25} (CH_3 rock)	0.148	b_2
ν_{26} (CH_2 rock)	0.093	b_2
ν_{27} (Torsion)	0.033	b_2

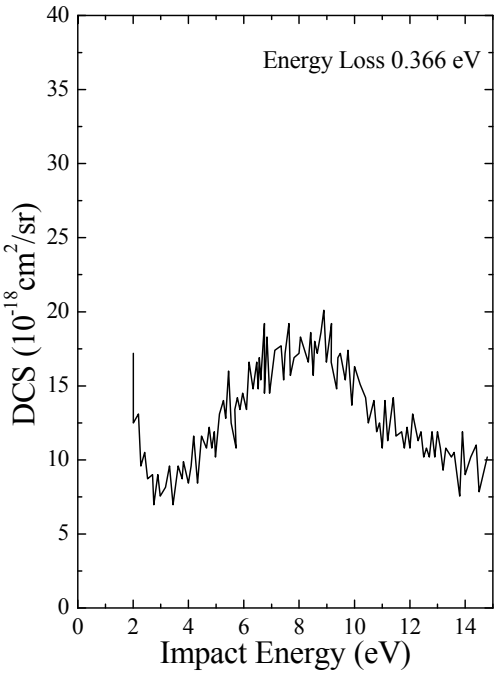

Figure A3.3. Vibrational excitation function of C_3H_8 at the scattering angle of 90 degrees.

Reference:

L. Boesten, M. A. Dillon, H. Tanaka, M. Kimura and H. Sato, *J. Phys. B* **27**, 1845 (1994).

A4. C_3H_6

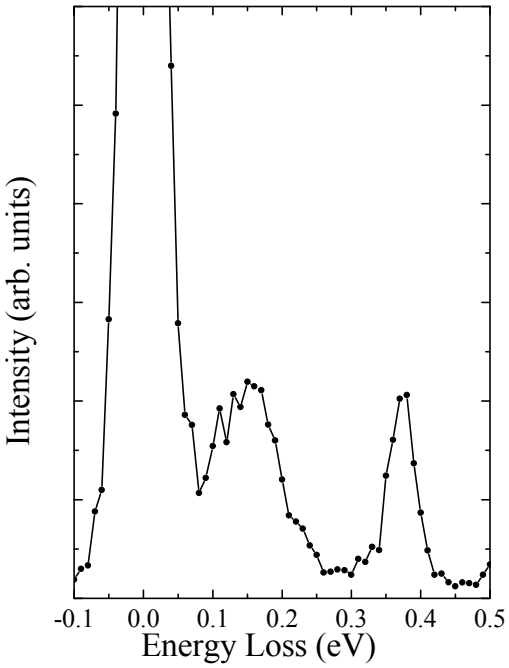

Figure A4.1. Energy loss spectrum of C_3H_6 at impact energy 10 eV for a scattering angle 90 degrees.

Table A4.1. Vibrational fundamental modes. (*NIST* Data Theory)

Vibrational mode	Energy (eV)	Species
ν_1	0.385	a'
ν_2	0.376	a'
ν_3	0.375	a'
ν_4	0.371	a'
ν_5	0.361	a'
ν_6	0.207	a'
ν_7	0.181	a'
ν_8	0.175	a'
ν_9	0.171	a'
ν_{10}	0.159	a'
ν_{11}	0.143	a'
ν_{12}	0.114	a'
ν_{13}	0.111	a'
ν_{14}	0.051	a'
ν_{15}	0.367	a"
ν_{16}	0.180	a"
ν_{17}	0.129	a"
ν_{18}	0.123	a"
ν_{19}	0.112	a"
ν_{20}	0.070	a"
ν_{21}	0.025	a"

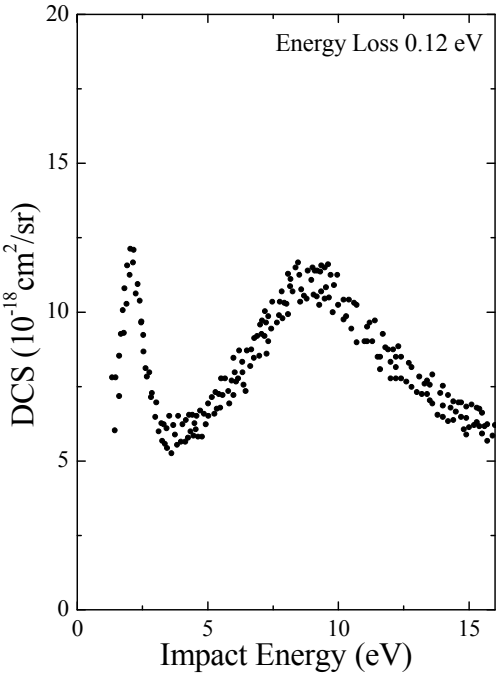

Figure A4.2. Vibrational excitation function of C_3H_6 at the scattering angle of 90 degrees.

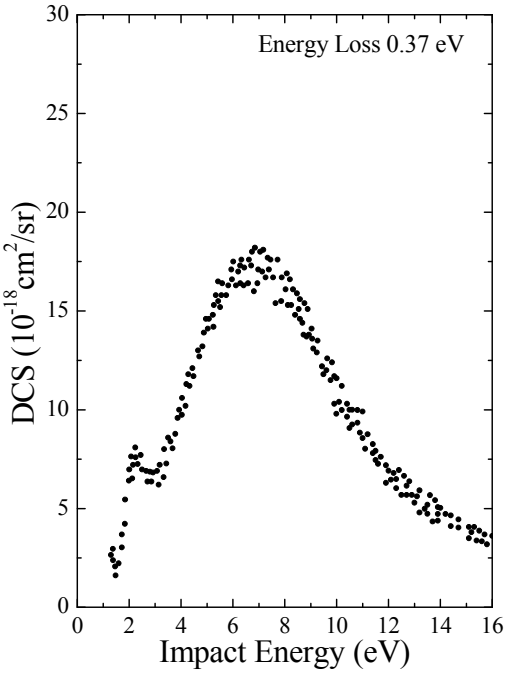

Figure A4.3. Vibrational excitation function of C_3H_6 at the scattering angle of 90 degrees.

Reference:

C. Makochekanwa, H. Kato, M. Hoshino, H. Cho, M. Kimura, O. Sueoka and H. Tanaka, *Eur. Phys. J. D* **35**, 249 (2005).

A5. *cyclo*-C_3H_6

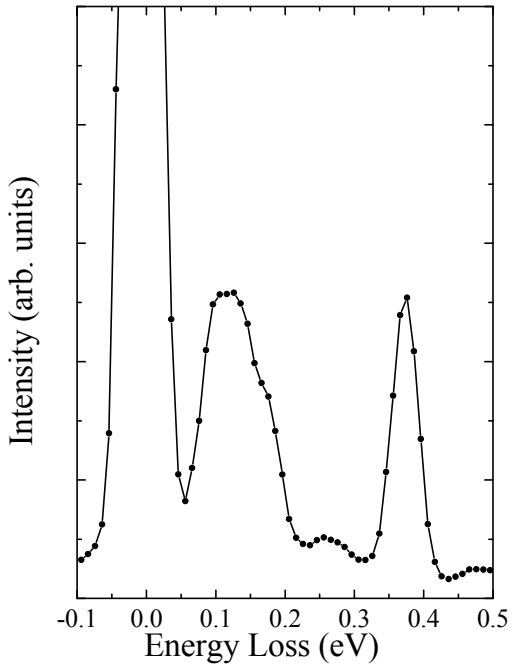

Figure A5.1. Energy loss spectrum of *cyclo*-C_3H_6 at impact energy 8 eV for a scattering angle 70 degrees.

Table A5.1. Vibrational fundamental modes.

Vibrational mode	Energy (eV)	Species
ν_1 (CH_2 s-str)	0.377	a_1'
ν_2 (CH_2 scis)	0.183	a_1'
ν_3 (Ring str)	0.147	a_1'
ν_4 (CH_2 twist)	0.140	a_1
ν_5 (CH_2 wag)	0.133	a_2'
ν_6 (CH_2 a-str)	0.385	a_2
ν_7 (CH_2 rock)	0.106	a_2
ν_8 (CH_2 s-str)	0.375	e'
ν_9 (CH_2 scis)	0.178	e'
ν_{10} (CH_2 wag)	0.128	e'
ν_{11} (Ring deform)	0.107	e'
ν_{12} (CH_2 a-str)	0.382	e
ν_{13} (CH_2 twist)	0.147	e
ν_{14} (CH_2 rock)	0.092	e

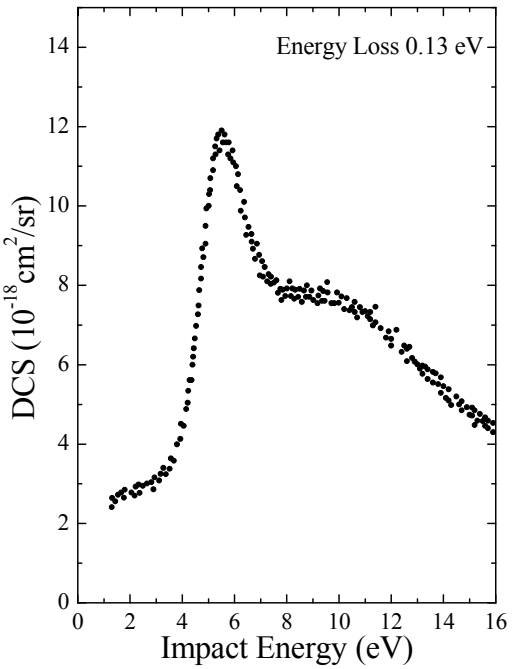

Figure A5.2. Vibrational excitation function of *cyclo*-C_3H_6 at the scattering angle of 90 degrees.

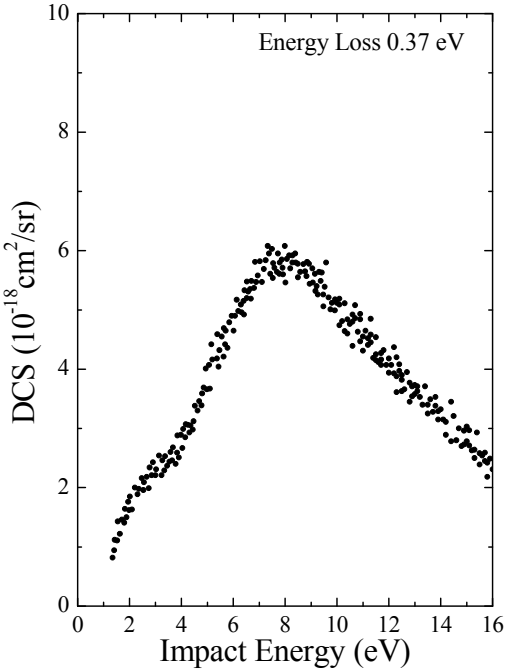

Figure A5.3. Vibrational excitation function of *cyclo*-C_3H_6 at the scattering angle of 90 degrees.

Reference:

C. Makochekanwa, H. Kato, M. Hoshino, H. Cho, M. Kimura, O. Sueoka and H. Tanaka, *Eur. Phys. J. D* **35**, 249 (2005).

A6. C_3H_4 (methylacetylene)

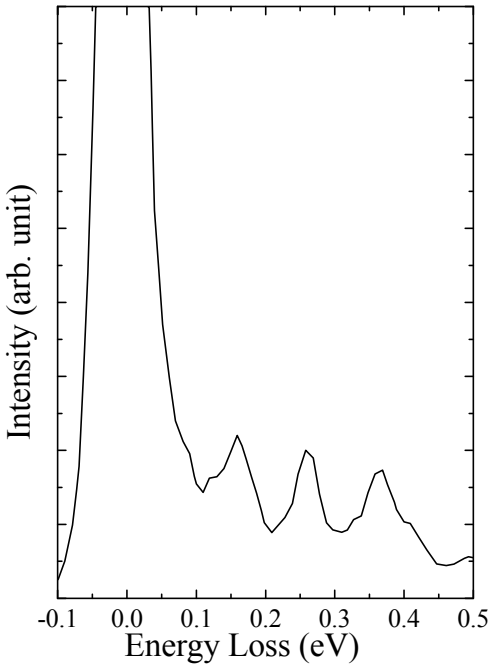

Figure A6.1. Energy loss spectrum of C_3H_4 at impact energy 3.2 eV for a scattering angle 120 degrees.

Table A6.1. Vibrational fundamental modes.

Vibrational mode	Energy (eV)	Species
ν_1 (CH str)	0.413	a_1
ν_2 (CH_3 s-str)	0.362	a_1
ν_3 (C≡C str)	0.266	a_1
ν_4 (CH_3 s-deform)	0.171	a_1
ν_5 (C-C str)	0.115	a_1
ν_6 (CH_3 d-str)	0.373	e
ν_7 (CH_3 d-deform)	0.180	e
ν_8 (CH_3 rock)	0.131	e
ν_9 (CH bend)	0.078	e
ν_{10} (CCC bend)	0.041	e

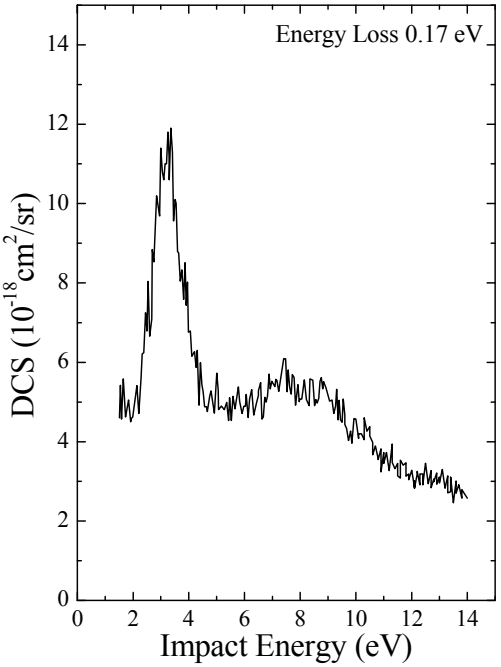

Figure A6.2. Vibrational excitation function of C_3H_4 at the scattering angle of 90 degrees.

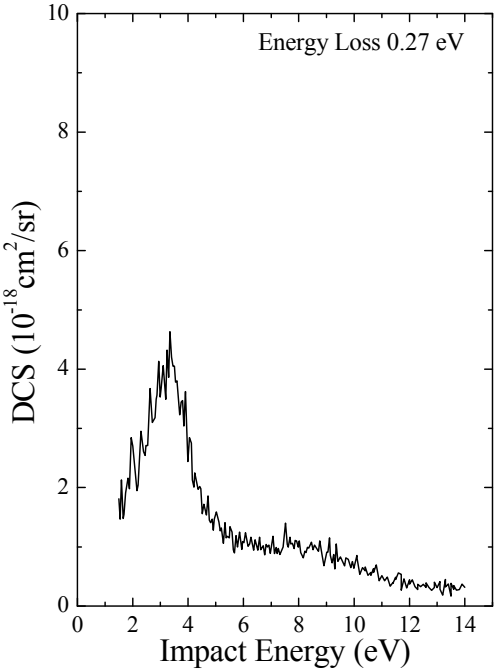

Figure A6.3. Vibrational excitation function of C_3H_4 at the scattering angle of 90 degrees.

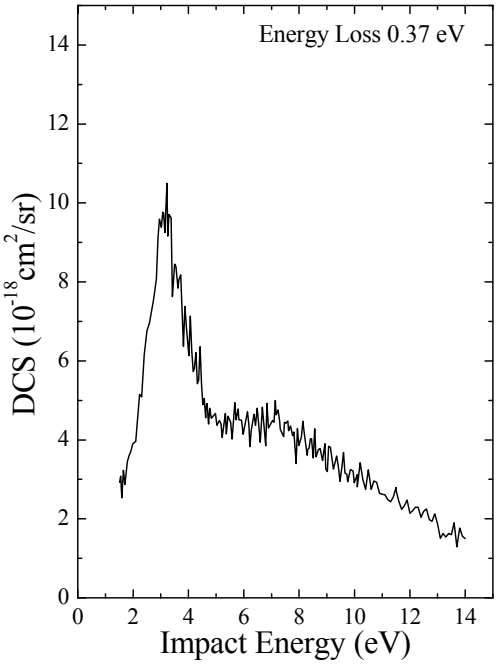

Figure A6.4. Vibrational excitation function of C_3H_4 at the scattering angle of 90 degrees.

Reference:

Y. Nakano, M. Hoshino, M. Kitajima and H. Tanaka, *Phys. Rev. A* **66**, 032714 (2002).

A7. C_3H_4 (Allene)

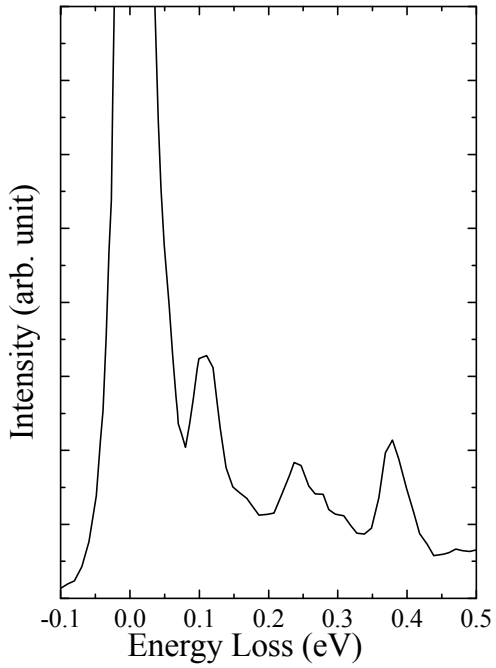

Figure A7.1. Energy loss spectrum of C_3H_4 at impact energy 2 eV for a scattering angle 90 degrees.

Table A7.1. Vibrational fundamental modes.

Vibrational mode	Energy (eV)	Species
ν_1 (CH_2 s-str)	0.374	a_1
ν_2 (CH_2 scis)	0.179	a_1
ν_3 (CC str)	0.133	a_1
ν_4 (CH_2 twist)	0.107	b_1
ν_5 (CH_2 s-str)	0.373	b_2
ν_6 (CC str)	0.243	b_2
ν_7 (CH_2 scis)	0.173	b_2
ν_8 (CH_2 a-str)	0.383	e
ν_9 (CH_2 rock)	0.124	e
ν_{10} (CH_2 wag)	0.104	e
ν_{11} (CCC deform)	0.044	e

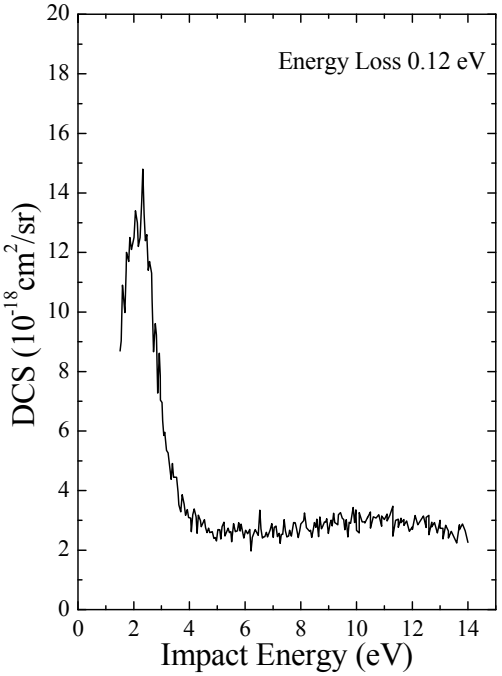

Figure A7.2. Vibrational excitation function of C_3H_4 at the scattering angle of 90 degrees.

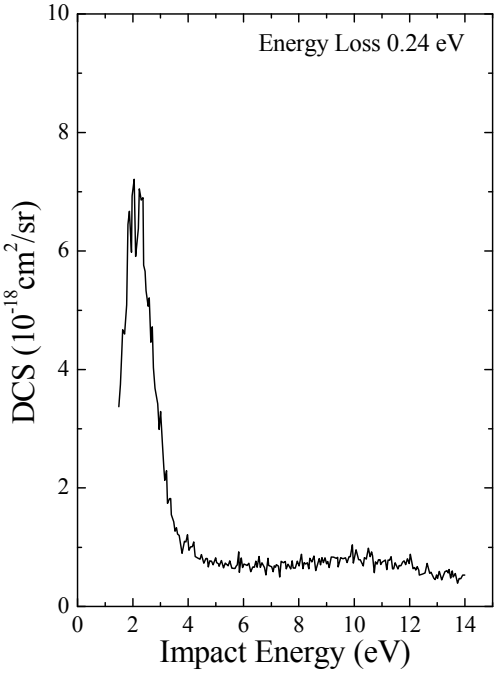

Figure A7.3. Vibrational excitation function of C_3H_4 at the scattering angle of 90 degrees.

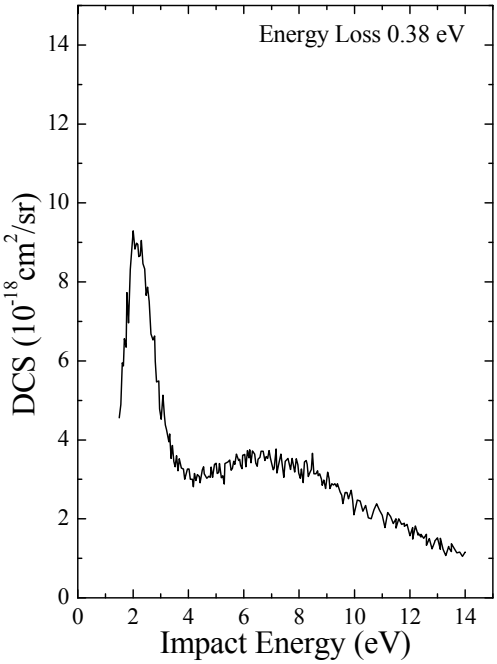

Figure A7.4. Vibrational excitation function of C_3H_4 at the scattering angle of 90 degrees.

Reference:

Y. Nakano, M. Hoshino, M. Kitajima and H. Tanaka, *Phys. Rev. A* **66**, 032714 (2002).

B. Processing Plasma-Related Gases

B1. $\underline{CF_4}$

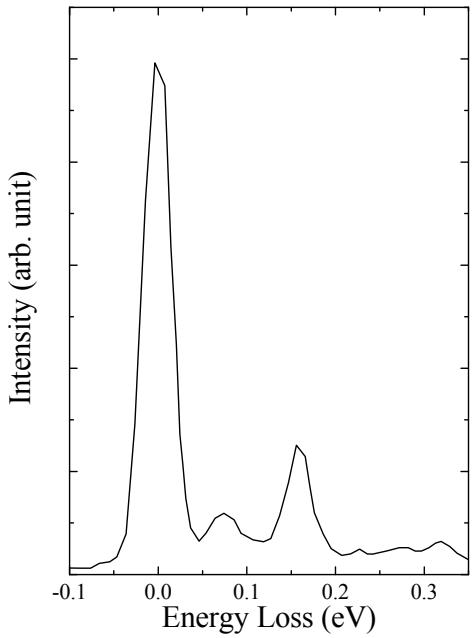

Figure B1.1. Energy loss spectrum of CF_4 at impact energy 8 eV for a scattering angle 90 degrees.

Table B1.1. Vibrational fundamental modes.

Vibrational mode	Energy (eV)	Species
ν_1 (Sym str)	0.113	a_1
ν_2 (Deg)	0.054	e
ν_3 (Deg str)	0.159	f_2
ν_4 (Deg deform)	0.078	f_2

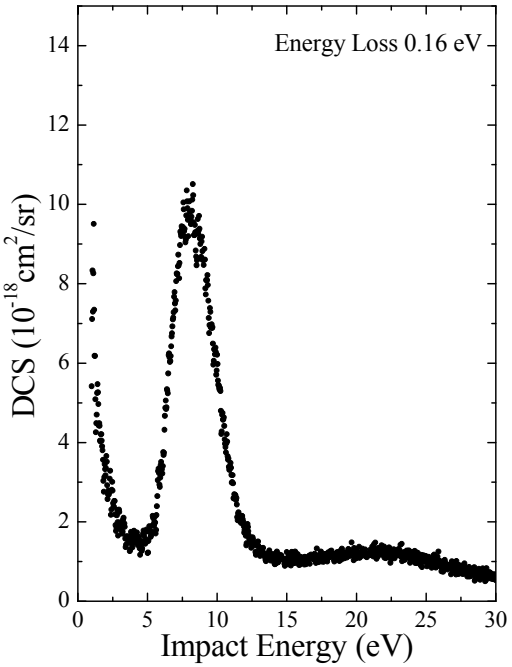

Figure B1.2. Vibrational excitation function of CF_4 at the scattering angle of 90 degrees.

Reference:

L. Boesten, H. Tanaka, A. Kobayashi, M. A. Dillon and M. Kimura, *J. Phys. B* **25**, 1607 (1992).

B2. C_2F_6

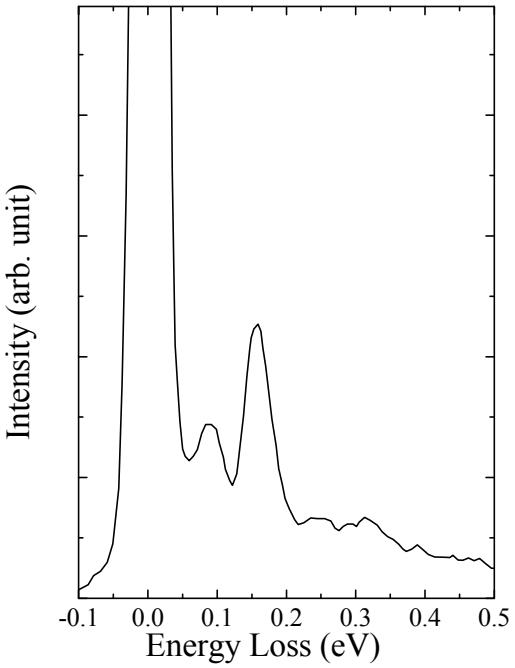

Figure B2.1. Energy loss spectrum of C_2F_6 at impact energy 8.5 eV for a scattering angle 90 degrees.

Table B2.1. Vibrational fundamental modes.

Vibrational mode	Energy (eV)	Species
ν_1 (CC str)	0.152	a_{1g}
ν_2 (CF_3 s-str)	0.100	a_{1g}
ν_3 (CF_3 s-deform)	0.043	a_{1g}
ν_4 (Torsion)	0.008	a_{1u}
ν_5 (CF_3 s-str)	0.138	a_{2u}
ν_6 (CF_3 s-deform)	0.089	a_{2u}
ν_7 (CF_3 d-str)	0.155	e_g
ν_8 (CF_3 d-deform)	0.077	e_g
ν_9 (CF_3 rock)	0.046	e_g
ν_{10} (CF_3 d-str)	0.155	e_u
ν_{11} (CF_3 d-deform)	0.064	e_u
ν_{12} (CF_3 rock)	0.027	e_u

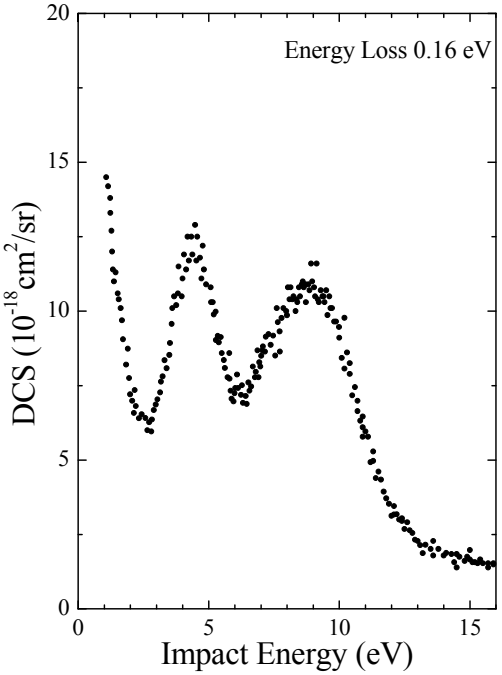

Figure B2.2. Vibrational excitation function of C_2F_6 at the scattering angle of 60 degrees.

Reference:

T. Takagi, L. Boesten, H. Tanaka and M. A. Dillon, *J. Phys. B* **27**, 5389 (1994).

B3. C_3F_8

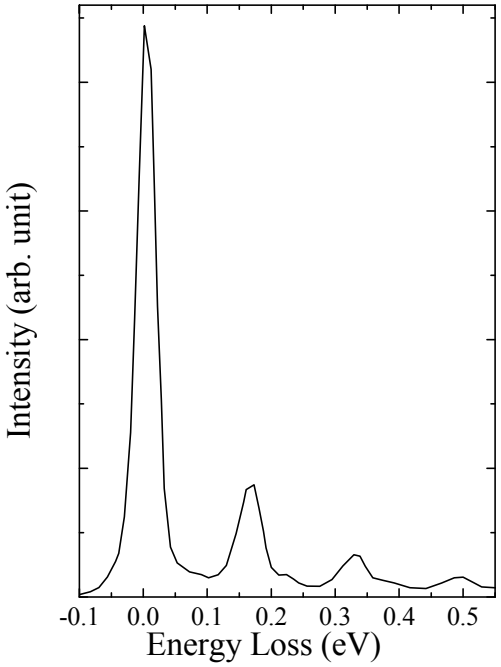

Figure B3.1. Energy loss spectrum of C_3F_8 at impact energy 3.0 eV for a scattering angle 120 degrees.

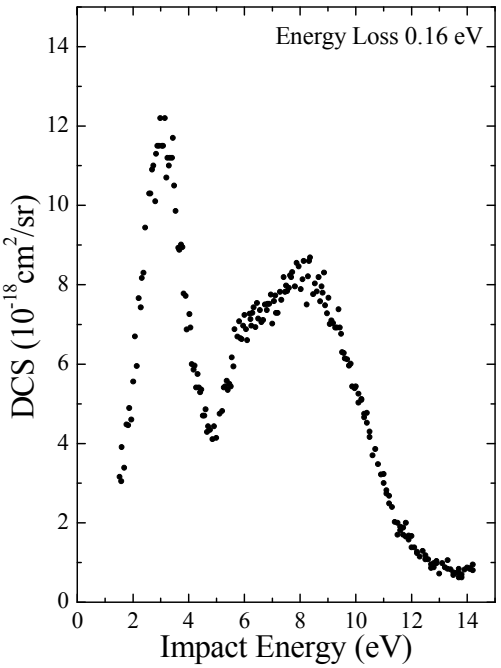

Figure B3.2. Vibrational excitation function of C_3F_8 at the scattering angle of 120 degrees.

Table B3.1. Vibrational fundamental modes.

Energy (eV)	Species
0.170	a_1
0.167	b_1
0.157	a_1
0.156	b_2
0.155	a_2
0.150	b_2
0.143	a_1
0.125	b_1
0.097	a_1
0.091	b_1
0.082	a_1
0.077	b_2
0.068	a_2
0.067	a_1
0.057	b_2
0.047	a_1
0.043	a_2
0.042	b_1
0.039	a_1
0.034	b_1
0.032	a_2
0.027	b_2
0.019	a_1

Reference:

H. Tanaka, Y. Tachibana, M. Kitajima, O. Sueoka, H. Takaki, A. Hamada and M. Kimura, *Phys. Rev. A* **59**, 2006 (1999).

B4. *cyclo*-C_4F_8

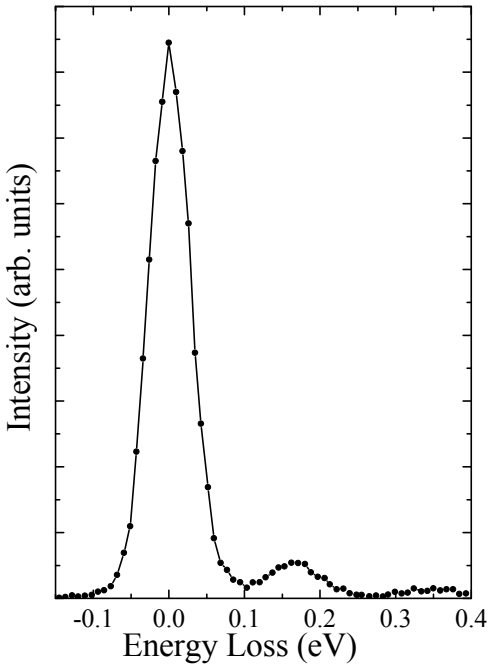

Figure B4.1. Energy loss spectrum of *cyclo*-C_4F_8 at impact energy 1.5 eV for a scattering angle 60 degrees.

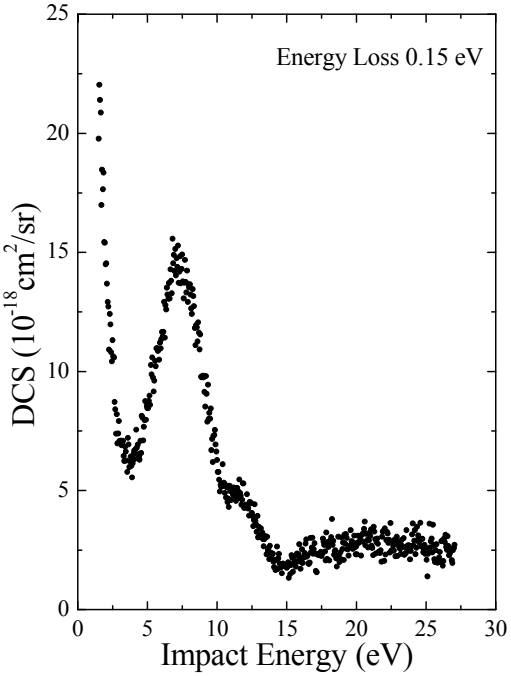

Figure B4.2. Vibrational excitation function of *cyclo*-C_4F_8 at the scattering angle of 50 degrees.

Table B4.1. Vibrational fundamental modes.

Vibrational mode	Energy (eV)	Species
CF str	0.177	a_{1g}
Ring str	0.087	a_{1g}
CF_2 deform	0.044	a_{1g}
CF_2 twist	0.021	a_{1u}
CF_2 wag	0.092	a_{2g}
CF str	0.154	a_{2u}
CF_2 rock	0.042	a_{2u}
CF str	0.151	b_{1g}
CF_2 wag	0.032	b_{1g}
CF str	0.172	b_{1u}
CF_2 rock	0.076	b_{1u}
out-of-plane ring bend	0.011	b_{1u}
CF str	0.125	b_{2g}
CF_2 deform	0.082	b_{2g}
in-plane ring bend	0.024	b_{2g}
CF_2 twist	0.031	b_{2u}
CF str	0.159	e_g
CF_2 rock	0.054	e_g
CF_2 twist	0.034	e_g
CF str	0.166	e_u
Ring str	0.119	e_u
CF_2 deform	0.071	e_u
CF_2 wag	0.035	e_u

Reference:

M. Jelisavcic, R. Panajotovic, M. Kitajima, M. Hoshino, H. Tanaka and S. J. Buckmana, *J. Chem. Phys.* **121**, 5272 (2004).

B5. C_2F_4

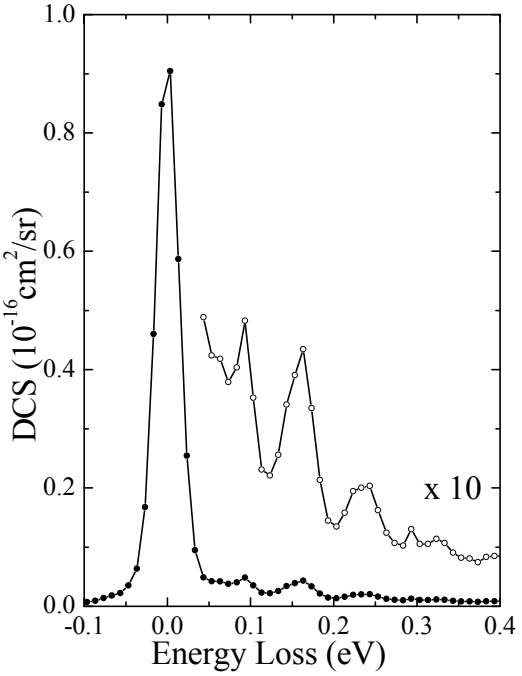

Figure B5.1. Energy loss spectrum of C_2F_4 at impact energy 8 eV for a scattering angle 90 degrees.

Table B5.1. Vibrational fundamental modes.

Vibrational mode	Energy (eV)	Species
ν_1 (CC str)	0.232	a_g
ν_2 (CF_2 s-str)	0.096	a_g
ν_3 (CF_2 scis)	0.049	a_g
ν_4 (CF_2 twist)	0.024	a_u
ν_5 (CF_2 a-str)	0.166	b_{1g}
ν_6 (CF_2 rock)	0.068	b_{1g}
ν_7 (CF_2 wag)	0.050	b_{1u}
ν_8 (CF_2 wag)	0.063	b_{2g}
ν_9 (CF_2 a-str)	0.166	b_{2u}
ν_{10} (CF_2 rock)	0.027	b_{2u}
ν_{11} (CF_2 s-str)	0.147	b_{3u}
ν_{12} (CF_2 scis)	0.069	b_{3u}

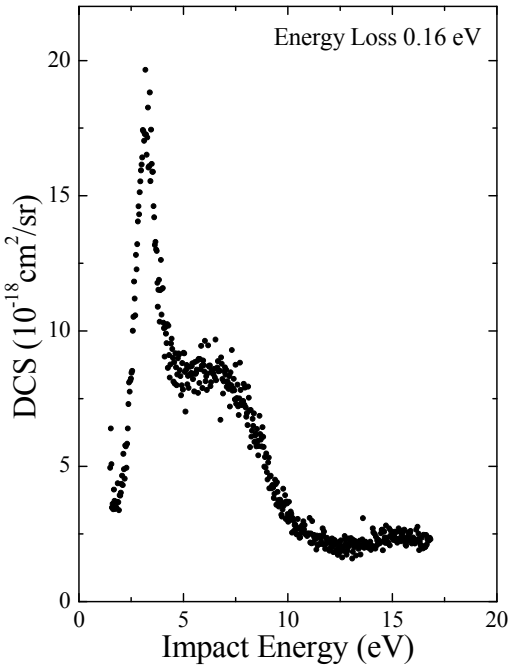

Figure B5.2. Vibrational excitation function of C_2F_4 at the scattering angle of 90 degrees.

Reference:

R. Panajotovic, M. Jelisavcic, R. Kajita, T. Tanaka, M. Kitajima, H. Cho, H. Tanaka and S.J. Buckman, J. Chem. Phys. **121**, 4559 (2004).

B6. C_6F_6

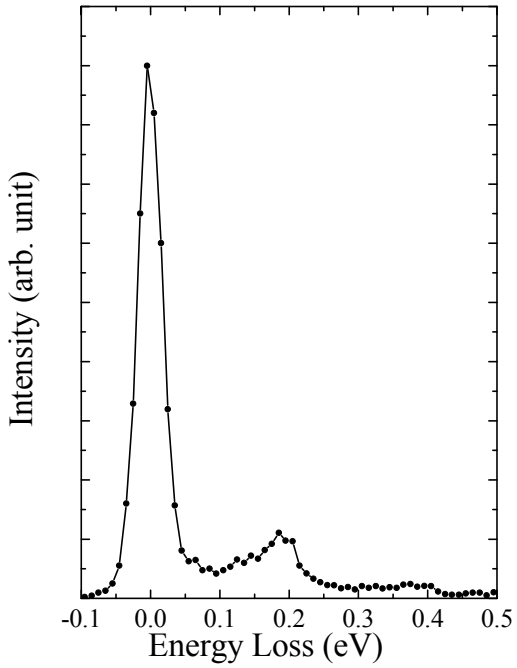

Figure B6.1. Energy loss spectrum of C_6F_6 at impact energy 5 eV for a scattering angle 90 degrees.

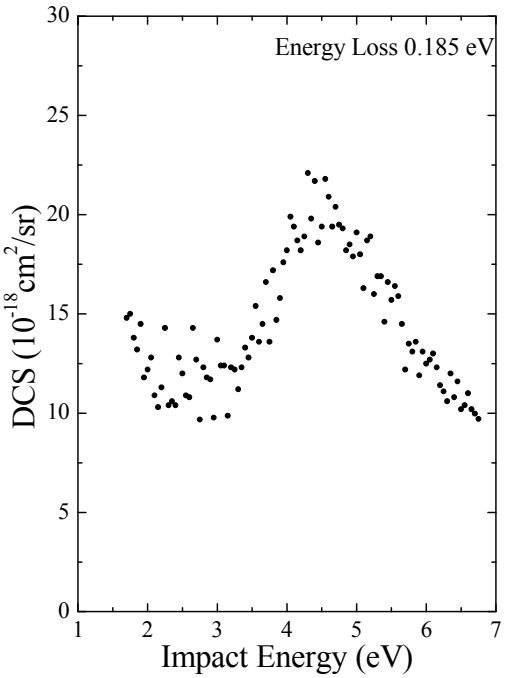

Figure B6.2. Vibrational excitation function of C_6F_6 at the scattering angle of 90 degrees.

Table B6.1. Vibrational fundamental modes.

Vibrational mode	Energy (eV)	Species
ν_1	0.185	a_{1g}
ν_2	0.069	a_{1g}
ν_3	0.086	a_{2g}
ν_4	0.027	a_{2u}
ν_5	0.164	b_{1u}
ν_6	0.079	b_{1u}
ν_7	0.089	b_{2g}
ν_8	0.031	b_{2g}
ν_9	0.155	b_{2u}
ν_{10}	0.026	b_{2u}
ν_{11}	0.046	e_{1g}
ν_{12}	0.190	e_{1u}
ν_{13}	0.125	e_{1u}
ν_{14}	0.039	e_{1u}
ν_{15}	0.205	e_{2g}
ν_{16}	0.143	e_{2g}
ν_{17}	0.055	e_{2g}
ν_{18}	0.033	e_{2g}
ν_{19}	0.074	e_{2u}
ν_{20}	0.022	e_{2u}

B7. C_3F_6

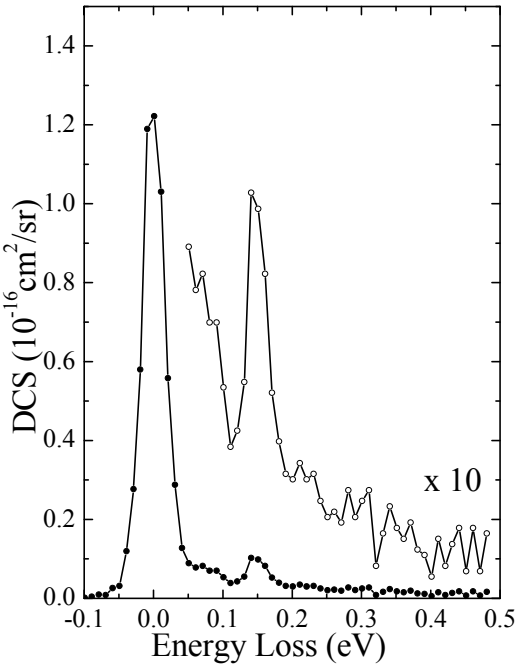

Figure B7.1. Energy loss spectrum of C_3F_6 at impact energy 8 eV for a scattering angle 90 degrees.

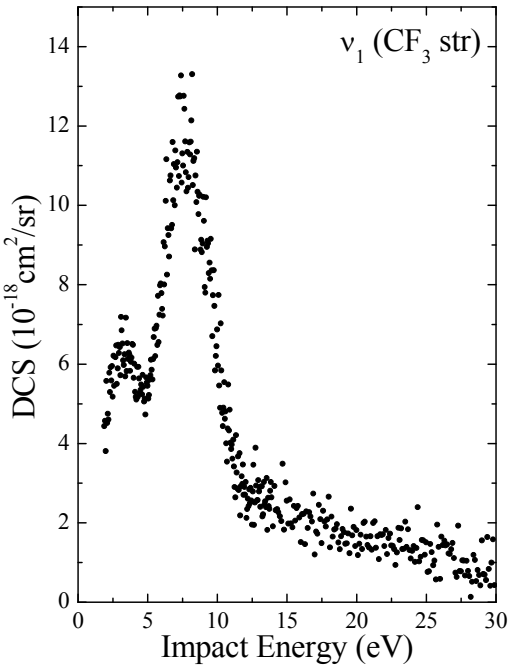

Figure B7.2. Vibrational excitation function of C_3F_6 at the scattering angle of 90 degrees.

Table B7.1. Vibrational fundamental modes.

Vibrational mode	Energy (eV)
C=C str	0.222
CF_3 s-str	0.172
CF_2 s-str	0.165
CF_3 a-str	0.150
CF_3 a-str	0.143
CF str	0.222
CF_2 a-str	0.126
CF_3 s-deform	0.095
CF_3 a-deform	0.089
CF_3 a-deform	0.080
CF_2 rock	0.075
CF_2 deform	0.069
CF_2 wag	0.063
CF_2 twist	0.045
C-C str	0.038
CF_3 bend	0.031
CF bend	0.026
CF_3 bend	0.021
CF bend	0.017
C-C=C bend	0.056
CF_3 twisting	0.010

B8. CH_3F

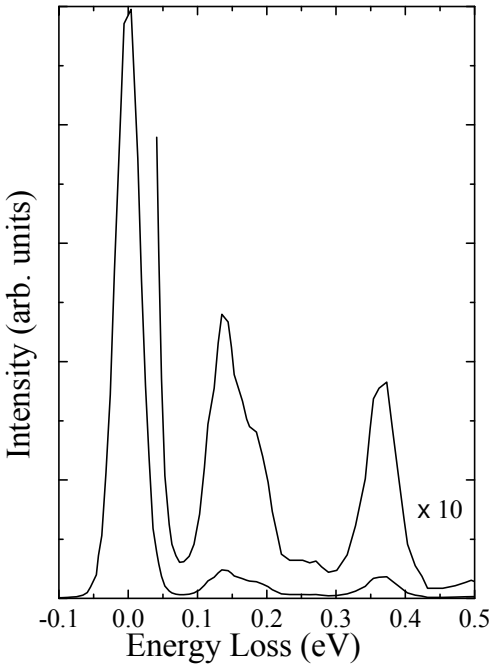

Figure B8.1. Energy loss spectrum of CH_3F at impact energy 8 eV for a scattering angle 90 degrees.

Table B8.1. Vibrational fundamental modes.

Vibrational mode	Energy (eV)	Species
ν_1 (CH_3 s-str)	0.363	a_1
ν_2 (CH_3 s-str)	0.363	a_1
ν_3 (CH_3 s-deform)	0.182	a_1
ν_4 (CF str)	0.130	a_1
ν_5 (CH_3 d-str)	0.373	e
ν_6 (CH_3 d-deform)	0.182	e
ν_7 (CH_3 rock)	0.147	e

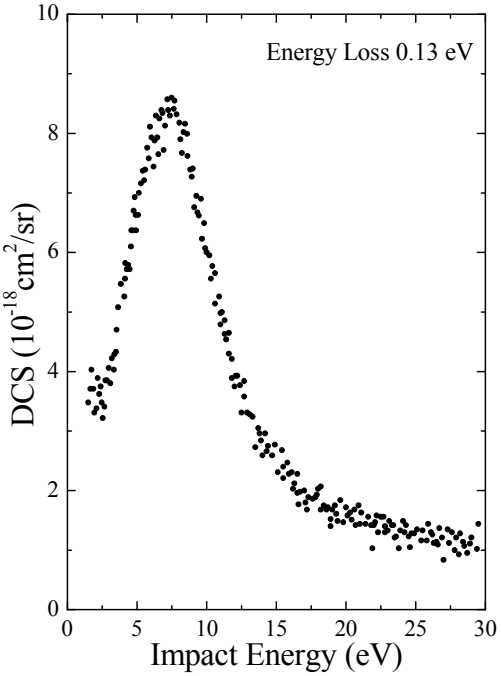

Figure B8.2. Vibrational excitation function of CH_3F at the scattering angle of 90 degrees.

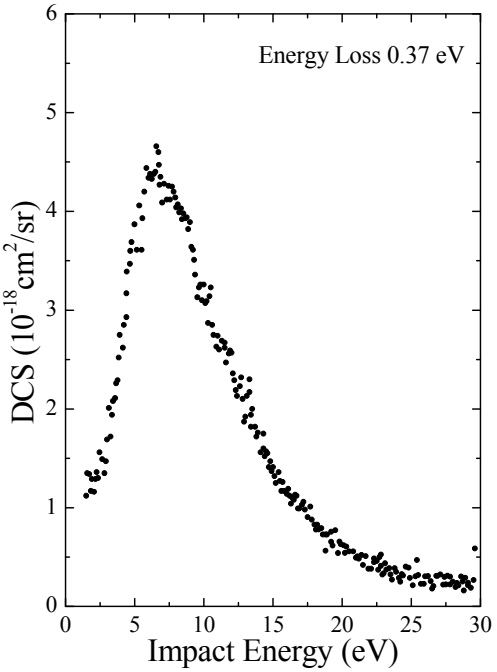

Figure B8.3. Vibrational excitation function of CH_3F at the scattering angle of 90 degrees.

B9. CH_2F_2

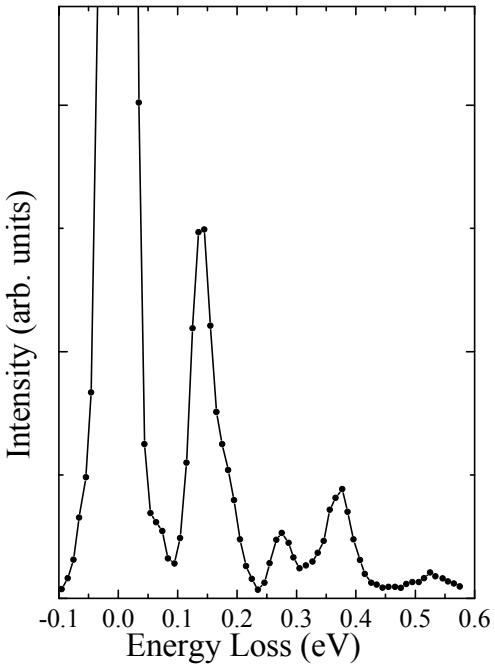

Figure B9.1. Energy loss spectrum of CH_2F_2 at impact energy 8 eV for a scattering angle 60 degrees.

Table B9.1. Vibrational fundamental modes. (*NIST* Data Theory)

Vibrational mode	Energy (eV)	Species
ν_1	0.364	a_1
ν_2	0.187	a_1
ν_3	0.135	a_1
ν_4	0.062	a_1
ν_5	0.152	a_2
ν_6	0.372	b_1
ν_7	0.142	b_1
ν_8	0.179	b_2
ν_9	0.134	b_2

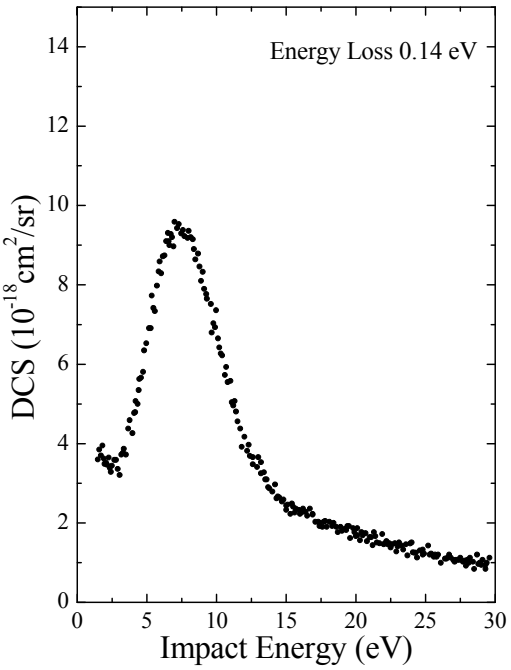

Figure B9.2. Vibrational excitation function of CH_2F_2 at the scattering angle of 90 degrees.

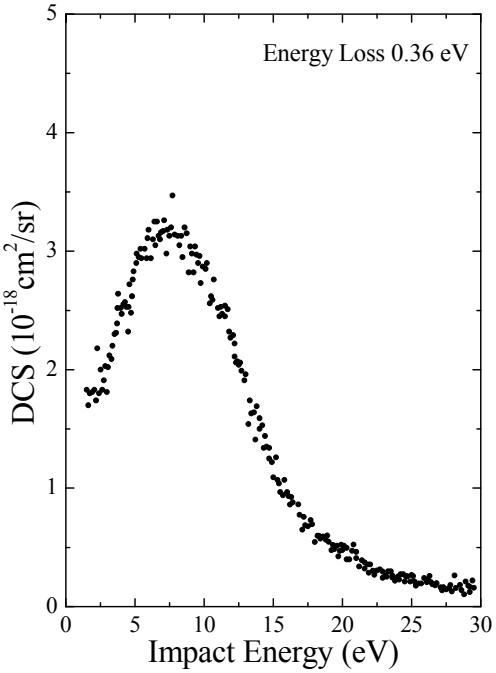

Figure B9.3. Vibrational excitation function of CH_2F_2 at the scattering angle of 90 degrees.

B10. CHF_3

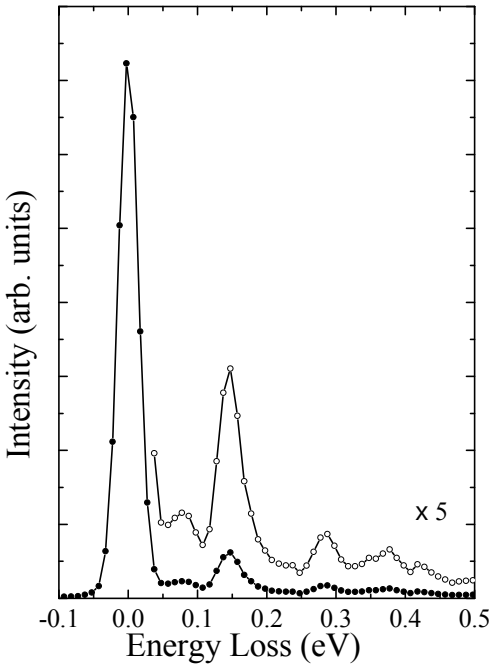

Figure B10.1. Energy loss spectrum of CHF_3 at impact energy 8 eV for a scattering angle 60 degrees.

Table B10.1. Vibrational fundamental modes.

Vibrational mode	Energy (eV)	Species
ν_1 (CH str)	0.376	a_1
ν_2 (CF_3 s-str)	0.138	a_1
ν_3 (CF_3 s-deform)	0.087	a_1
ν_4 (CH bend)	0.170	e
ν_5 (CF_3 d-str)	0.143	e
ν_6 (CF_3 d-deform)	0.063	e

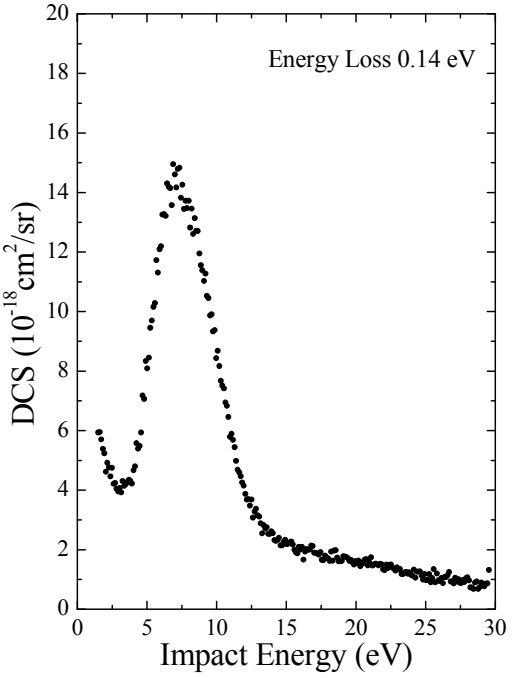

Figure B10.2. Vibrational excitation function of CHF_3 at the scattering angle of 90 degrees.

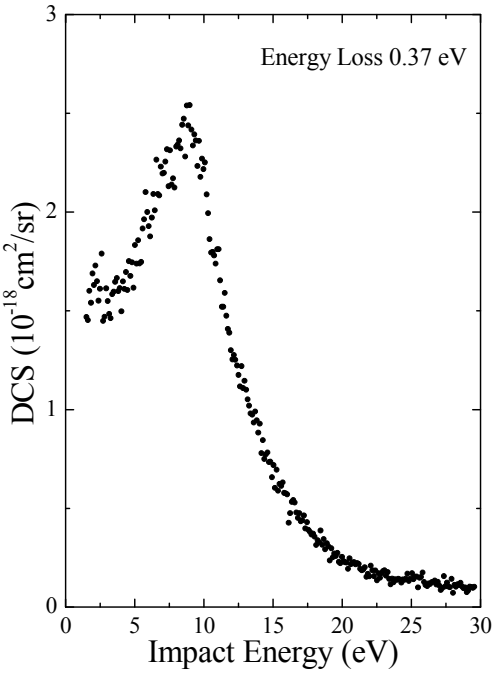

Figure B10.3. Vibrational excitation function of CHF_3 at the scattering angle of 90 degrees.

Reference:

K. Sunohara, M. Kitajima, H. Tanaka, M. Kimura and H. Cho, *J. Phys. B* **36**, 1843 (2003).

B11. $\underline{NF_3}$

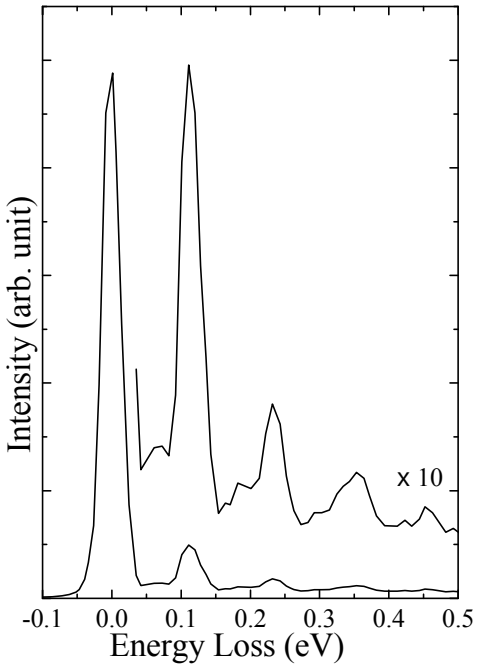

Figure B11.1. Energy loss spectrum of NF_3 at impact energy 3 eV for a scattering angle 60 degrees.

Table B11.1. Vibrational fundamental modes.

Vibrational mode	Energy (eV)	Species
ν_1 (Sym str)	0.128	a_1
ν_2 (Sym deform)	0.080	a_1
ν_3 (Deg str)	0.112	e
ν_4 (Deg deform)	0.061	e

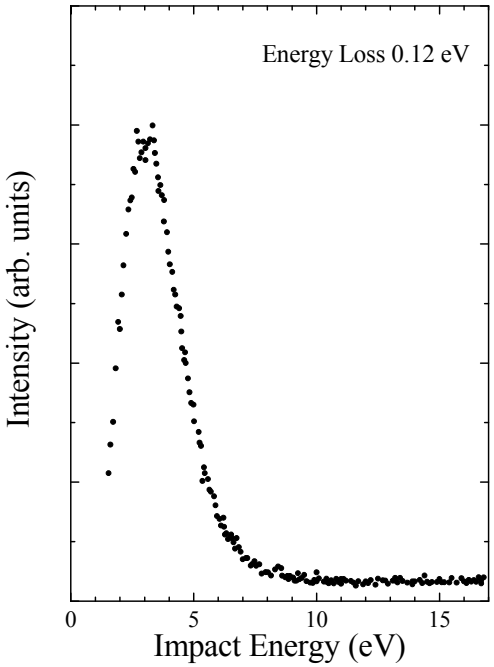

Figure B11.2. Vibrational excitation function of NF_3 at the scattering angle of 90 degrees.

Reference:

L. Boesten, Y. Tachibana, Y. Nakano, T. Shinohara, H. Tanaka and M. A. Dillon, *J. Phys. B* **29**, 5475 (1996).

B12. SiH_4

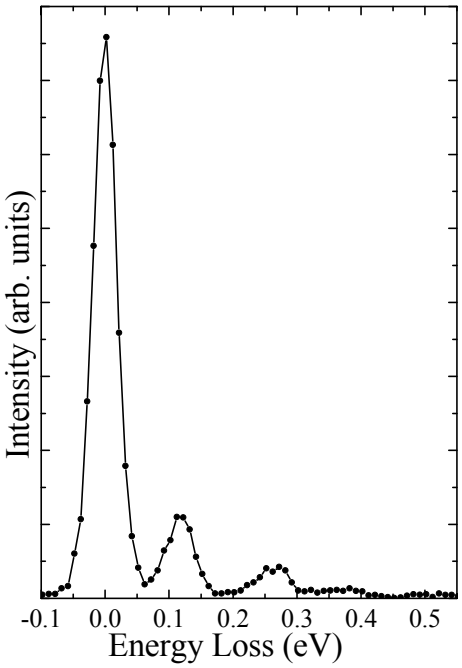

Figure B12.1. Energy loss spectrum of SiH_4 at impact energy 2.5 eV for a scattering angle 80 degrees.

Table B12.1. Vibrational fundamental modes.

Vibrational mode	Energy (eV)	Species
ν_1 (Sym str)	0.271	a_1
ν_2 (Deg deform)	0.121	e
ν_3 (Deg str)	0.272	f_2
ν_4 (Deg deform)	0.113	f_2

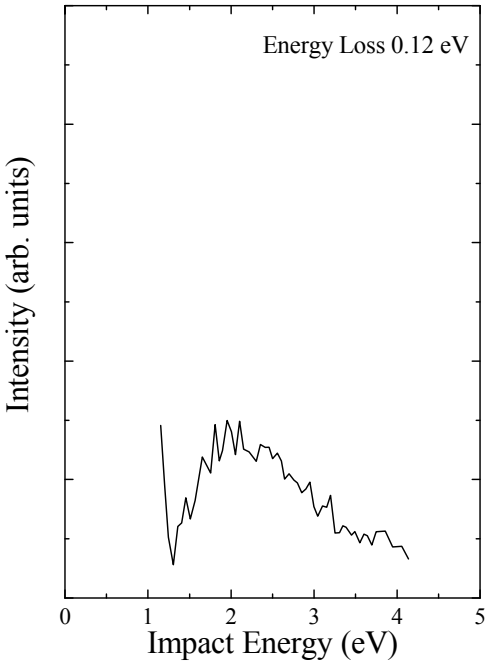

Figure B12.2. Vibrational excitation function of SiH_4 at the scattering angle of 90 degrees.

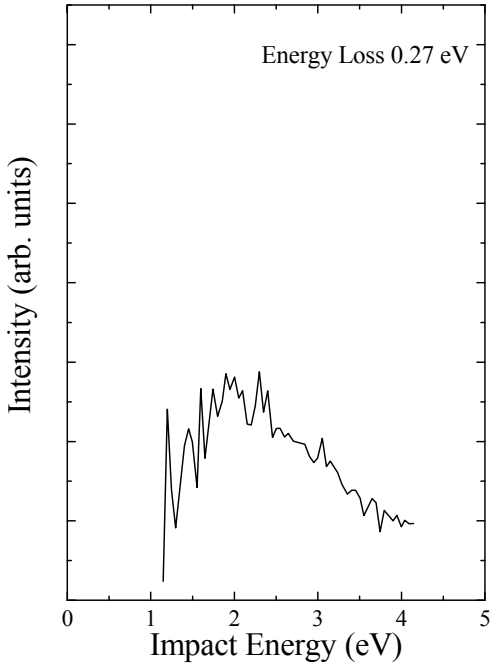

Figure B12.3. Vibrational excitation function of SiH_4 at the scattering angle of 90 degrees.

Reference:

H. Tanaka, L. Boesten, H. Sato, M. Kimura, M. A. Dillon and D. Spence, *J. Phys. B* **23**, 577 (1990).

B13. Si_2H_6

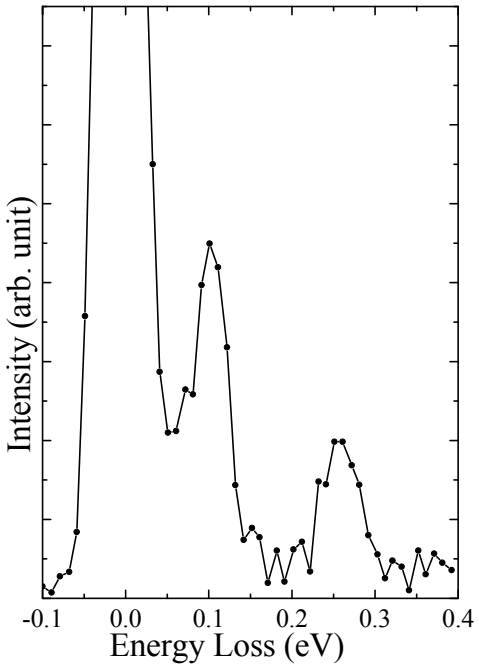

Figure B13.1. Energy loss spectrum of Si_2H_6 at impact energy 2 eV for a scattering angle 80 degrees.

Table B13.1. Vibrational fundamental modes.

Vibrational mode	Energy (eV)	Species
ν_1	0.267	a_{1g}
ν_2	0.113	a_{1g}
ν_3	0.054	a_{1g}
ν_4	0.016	a_{1u}
ν_5	0.267	a_{2u}
ν_6	0.105	a_{2u}
ν_7	0.267	e_g
ν_8	0.115	e_g
ν_9	0.078	e_g
ν_{10}	0.270	e_u
ν_{11}	0.116	e_u
ν_{12}	0.047	e_u

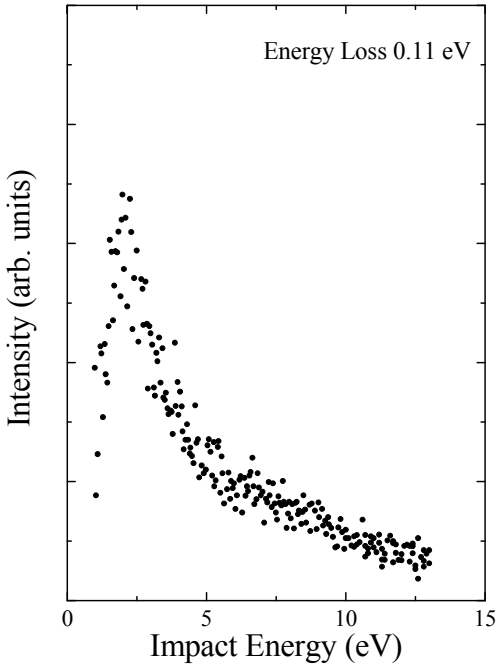

Figure B13.2. Vibrational excitation function of Si_2H_6 at the scattering angle of 40 degrees.

Reference:

M. A. Dillon, L. Boesten, H. Tanaka, M. Kimura and H. Sato, *J. Phys. B* **27**, 1209 (1994).

B14. GeH_4

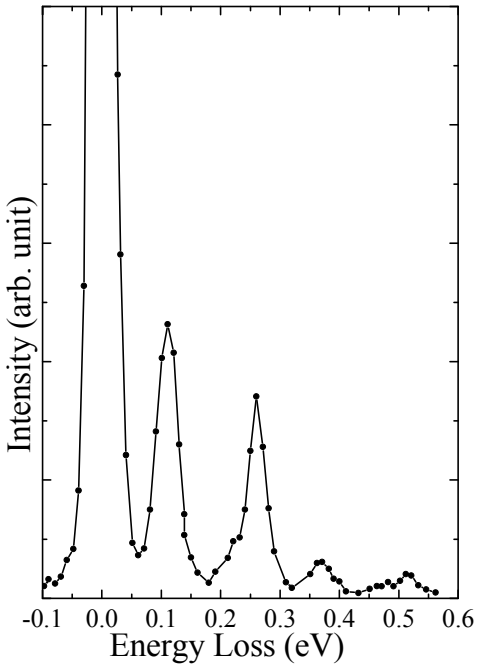

Figure B14.1. Energy loss spectrum of GeH_4 at impact energy 2.25 eV for a scattering angle 80 degrees.

Table B14.1. Vibrational fundamental modes.

Vibrational mode	Energy (eV)	Species
ν_1 (Sym str)	0.261	a_1
ν_2 (Deg deform)	0.115	e
ν_3 (Deg str)	0.262	f_2
ν_4 (Deg deform)	0.102	f_2

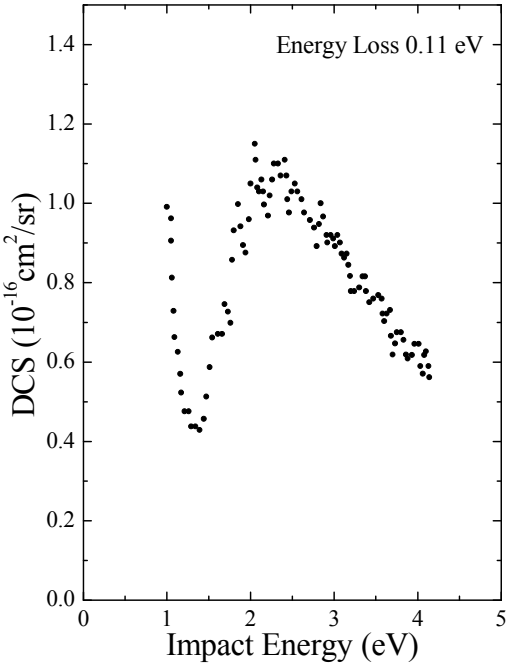

Figure B14.2. Vibrational excitation function of GeH_4 at the scattering angle of 90 degrees.

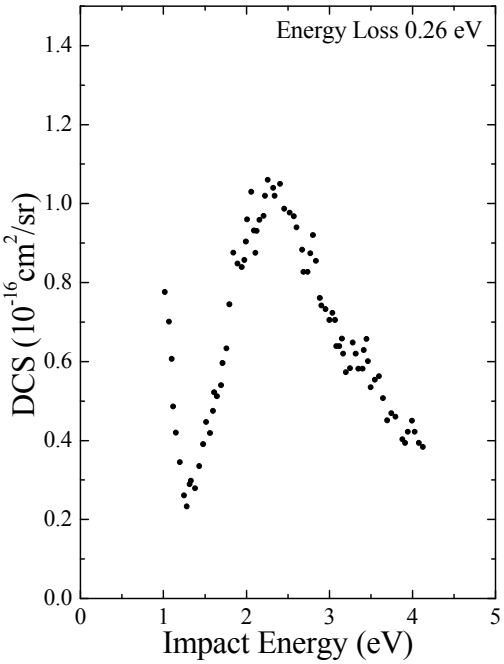

Figure B14.3. Vibrational excitation function of GeH_4 at the scattering angle of 90 degrees.

Reference:

M. A. Dillon, L. Boesten, H. Tanaka, M. Kimura and H. Sato, *J. Phys. B* **26**, 3147 (1993).

B15. SiF_4

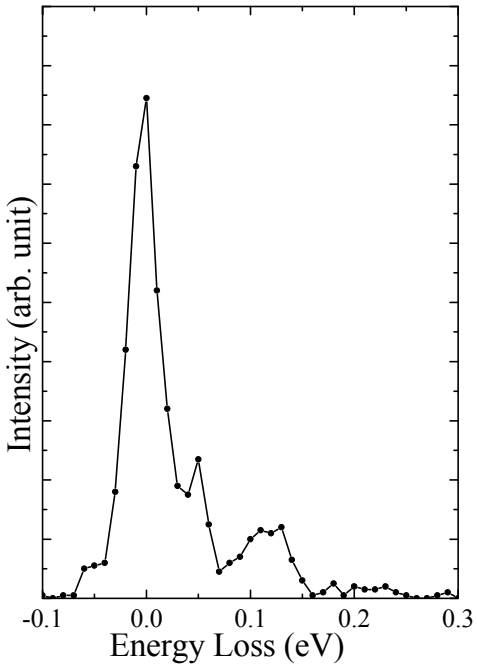

Figure B15.1. Energy loss spectrum of SiF_4 at impact energy 5 eV for a scattering angle 30 degrees.

Table B15.1. Vibrational fundamental modes.

Vibrational mode	Energy (eV)	Species
ν_1 (Sym str)	0.099	a_1
ν_2 (Deg deform)	0.033	e
ν_3 (Deg str)	0.128	f_2
ν_4 (Deg deform)	0.048	f_2

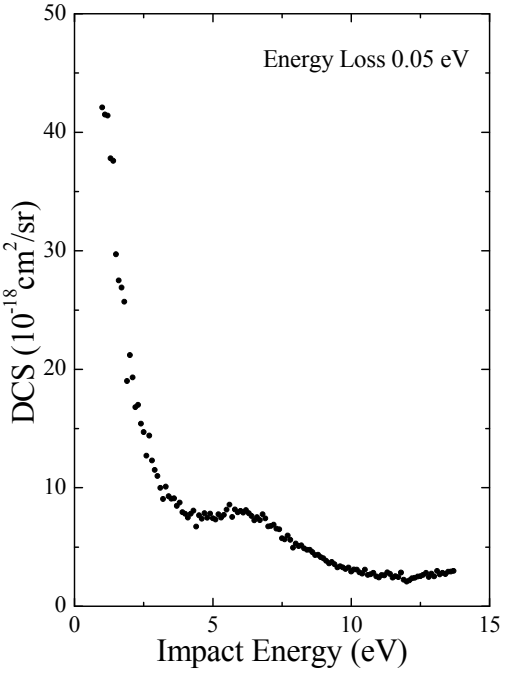

Figure B15.2. Vibrational excitation function of SiF_4 at the scattering angle of 60 degrees.

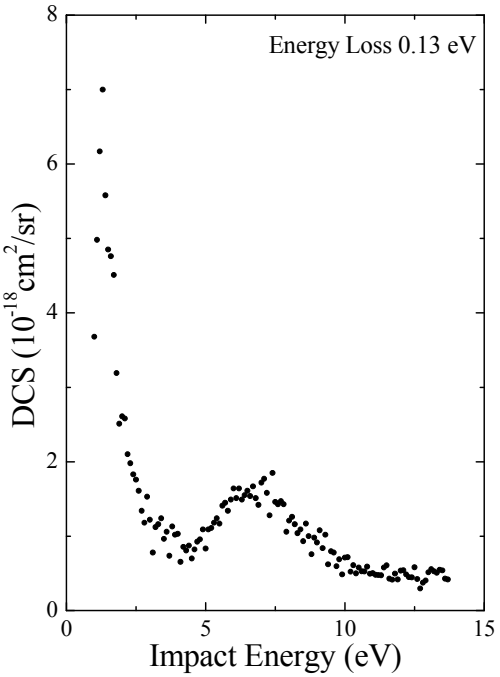

Figure B15.3. Vibrational excitation function of SiF_4 at the scattering angle of 60 degrees.

B16. F_2CO

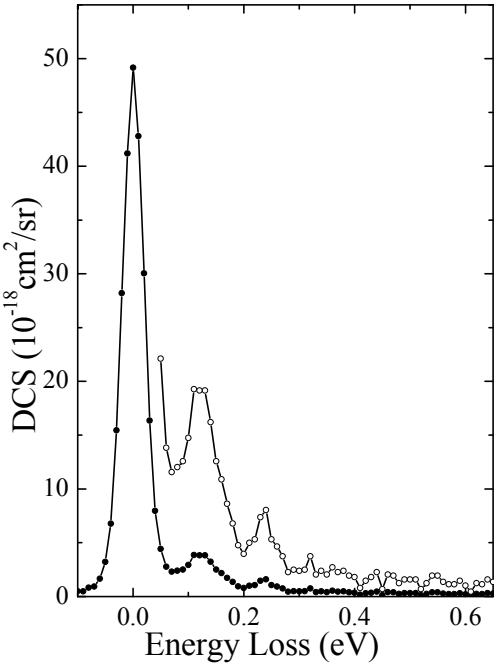

Figure B16.1. Energy loss spectrum of F_2CO at impact energy 7.5 eV for a scattering angle 90 degrees.

Table B16.1. Vibrational fundamental modes.

Vibrational mode	Energy (eV)	Species
ν_1 (CO str)	0.239	a_1
ν_2 (CF_2 s-str)	0.12	a_1
ν_3 (CF_2 scis)	0.072	a_1
ν_4 (CF_2 a-str)	0.155	b_1
ν_5 (CF_2 rock)	0.078	b_1
ν_6 (CF_2 wag)	0.096	b_2

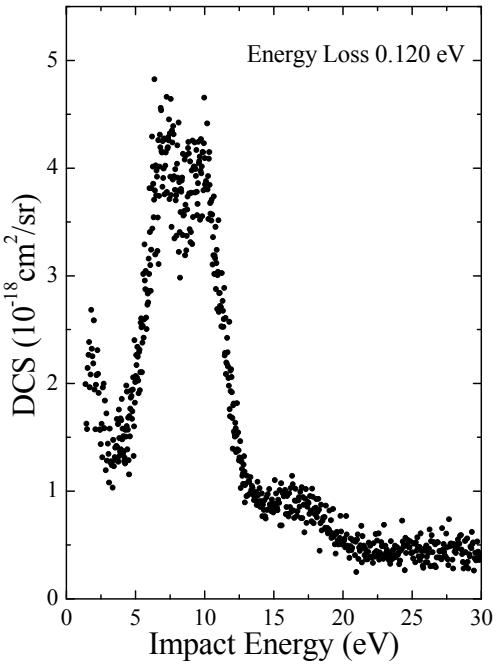

Figure B16.2. Vibrational excitation function of F_2CO at the scattering angle of 90 degrees.

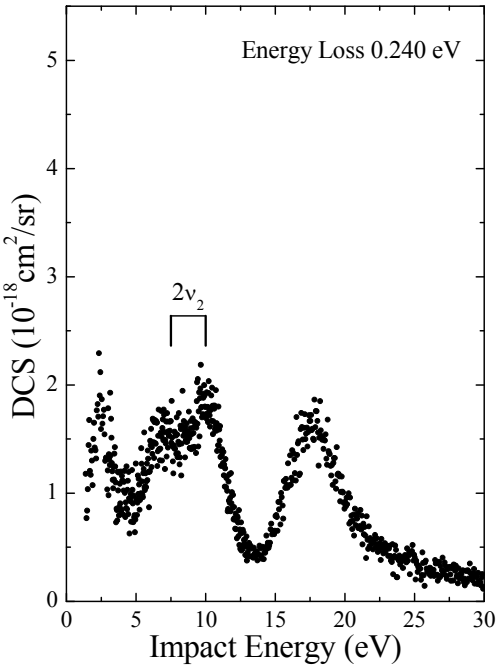

Figure B16.3. Vibrational excitation function of F_2CO at the scattering angle of 90 degrees.

Reference:

H. Kato, C. Makochekanwa, M. Hoshino, M. Kimura, H. Cho, T. Kume, A. Yamamoto, H. Tanaka, *Chem. Phys. Lett.* **425**, 1 (2006).

C. Environmental Issues -Related Gases

C1. $\underline{CF_3Cl}$

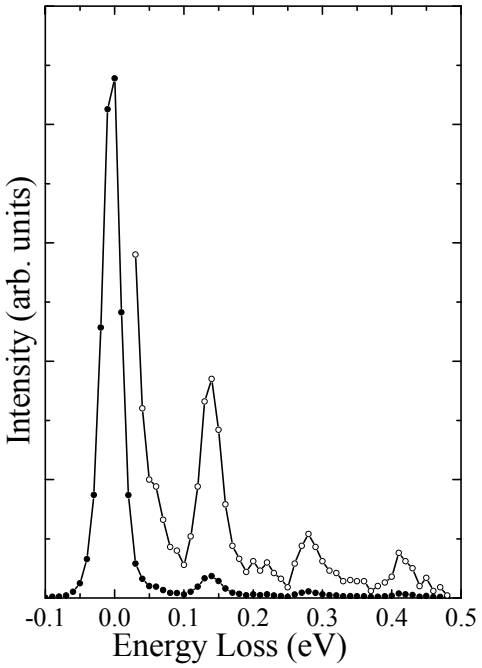

Figure C1.1. Energy loss spectrum of CF_3Cl at impact energy 5 eV for a scattering angle 60 degrees.

Table C1.1. Vibrational fundamental modes.

Vibrational mode	Energy (eV)	Species
ν_1 (CF_3 s-str)	0.137	a_1
ν_2 (CCl str)	0.097	a_1
ν_3 (CF_3 s-deform)	0.059	a_1
ν_4 (CF_3 d-str)	0.150	e
ν_5 (CF_3 d-deform)	0.070	e
ν_6 (CCl bend)	0.043	e

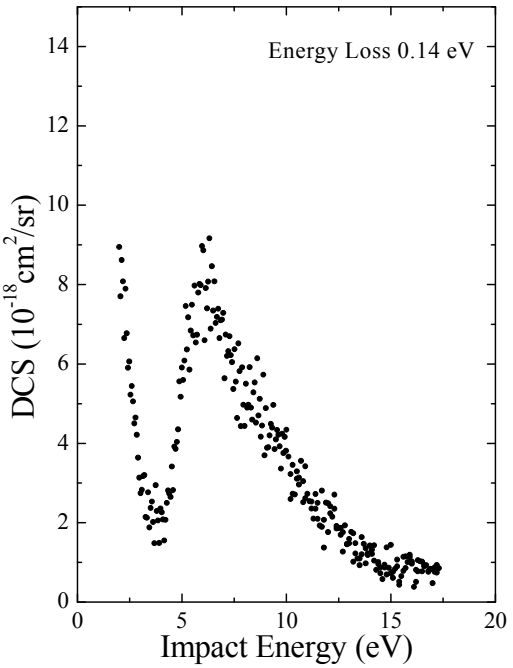

Figure C1.2. Vibrational excitation function of CF_3Cl at the scattering angle of 60 degrees.

Reference:

K. Sunohara, M. Kitajima, H. Tanaka, M. Kimura and H. Cho, *J. Phys. B* **36**, 1843 (2003).

C2. CF_3Br

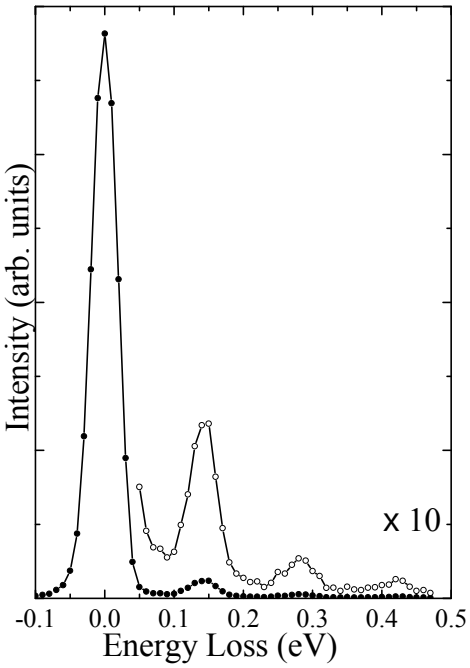

Figure C2.1. Energy loss spectrum of CF_3Br at impact energy 5 eV for a scattering angle 30 degrees.

Table C2.1. Vibrational fundamental modes.

Vibrational mode	Energy (eV)	Species
ν_1 (CF_3 s-str)	0.135	a_1
ν_2 (CF_3 s-deform)	0.094	a_1
ν_3 (CBr str)	0.043	a_1
ν_4 (CF_3 d-str)	0.150	e
ν_5 (CF_3 d-deform)	0.068	e
ν_6 (CBr bend)	0.038	e

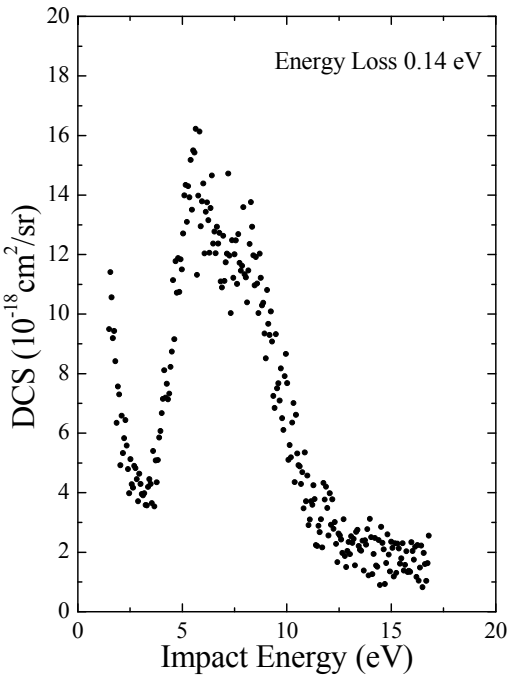

Figure C2.2. Vibrational excitation function of CF_3Br at the scattering angle of 60 degrees.

Reference:

K. Sunohara, M. Kitajima, H. Tanaka, M. Kimura and H. Cho, *J. Phys. B* **36**, 1843 (2003).

C3. CF_3I

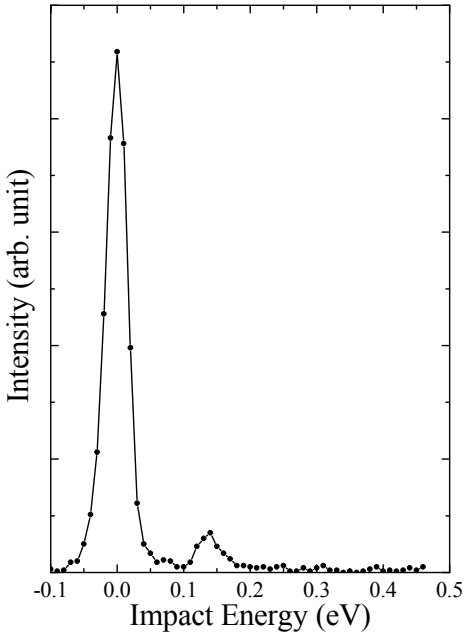

Figure C3.1. Energy loss spectrum of CF_3I at impact energy 4 eV for a scattering angle 60 degrees.

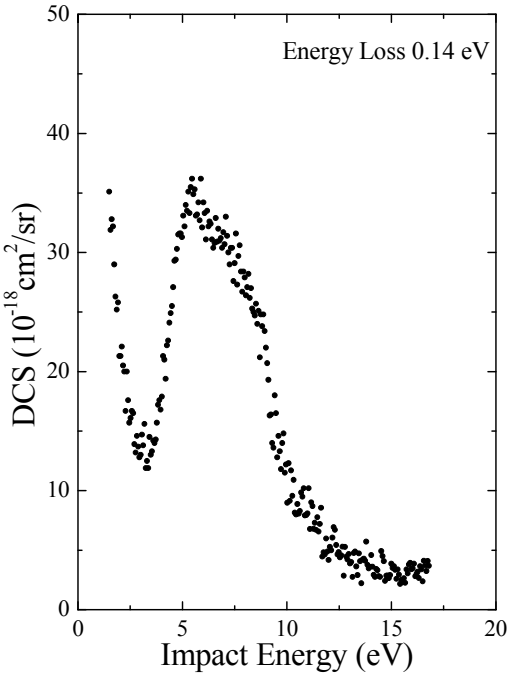

Figure C3.2. Vibrational excitation function of CF_3I at the scattering angle of 60 degrees.

Table C3.1. Vibrational fundamental modes.

Vibrational mode	Energy (eV)	Species
ν_1 (CF_3 s-str)	0.134	a_1
ν_2 (CF_3 s-deform)	0.092	a_1
ν_3 (CI str)	0.035	a_1
ν_4 (CF_3 d-str)	0.147	e
ν_5 (CF_3 d-deform)	0.067	e
ν_6 (CI bend)	0.032	e

Reference:

M. Kitajima, M. Okamoto, K. Sunohara, H. Tanaka, H. Cho, S. Samukawa, S. Eden and N. J. Mason, *J. Phys. B* **35**, 3257 (2002).

C4. $\underline{CO_2}$

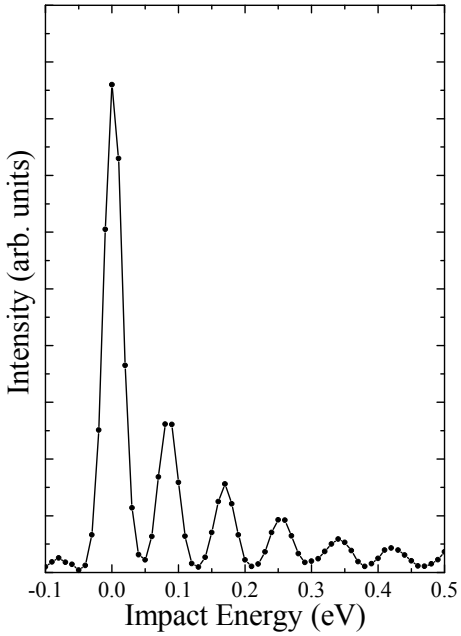

Figure C4.1. Energy loss spectrum of CO_2 at impact energy 3.8 eV for a scattering angle 80 degrees.

Table C4.1. Vibrational fundamental modes.

Vibrational mode	Energy (eV)	Species
ν_1 (100), s-str	0.165	σ_g
ν_2 (001), a-str	0.291	σ_u
ν_3 (010), bend	0.083	π_u

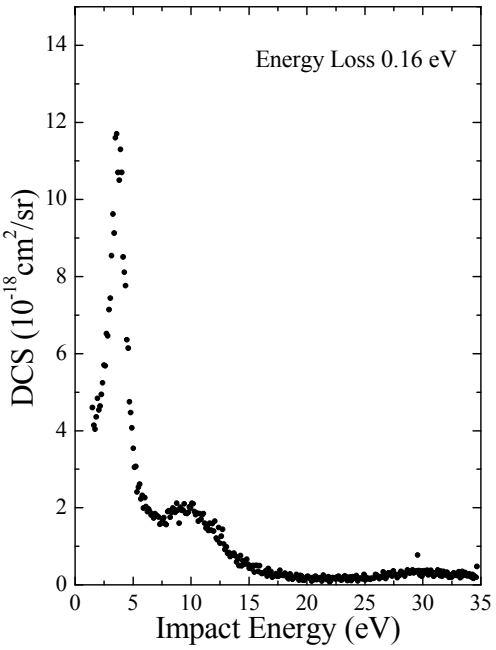

Figure C4.2. Vibrational excitation function of CO_2 at the scattering angle of 90 degrees.

Reference:

M. Kitajima, S. Watanabe, H. Tanaka, M. Kimura and Y. Ictikawa, *J. Phys. B* **34**, 1929 (2001).

C5. N_2O

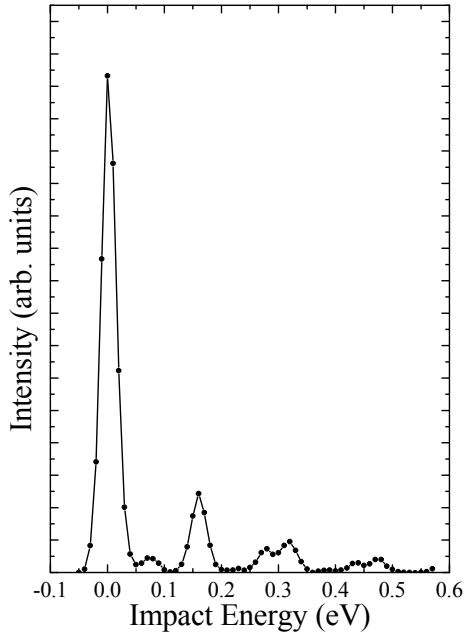

Figure C5.1. Energy loss spectrum of N_2O at impact energy 2.2 eV for a scattering angle 30 degrees.

Table C5.1. Vibrational fundamental modes.

Vibrational mode	Energy (eV)	Species
ν_1 (NN str)	0.276	σ^+
ν_2 (bend)	0.073	π
ν_3 (NO str)	0.159	σ^+

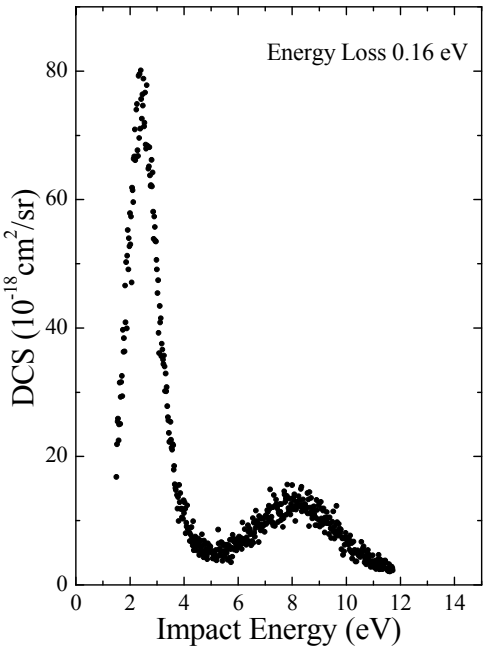

Figure C5.2. Vibrational excitation function of N_2O at the scattering angle of 30 degrees.

Reference:

K. Kitajima, Y. Sakamoto, R. J. Gulley, M. Hoshino, J. G. Gibson, H. Tanaka and S. J. Buckman, *J. Phys. B* **33**, 1687 (2000).

C6. CO

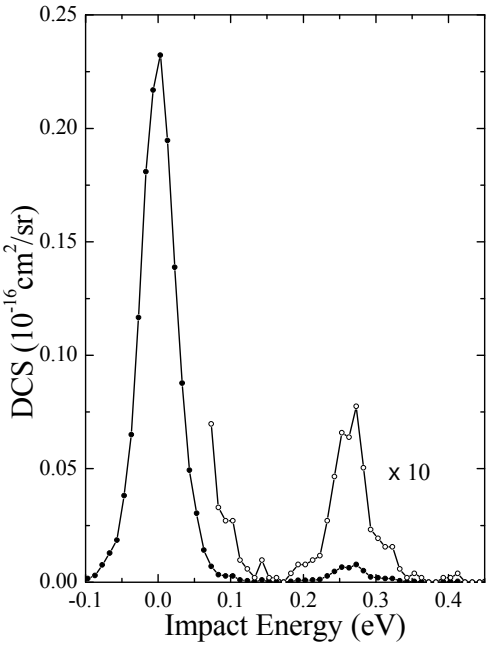

Figure C6.1. Energy loss spectrum of CO at impact energy 20 eV for a scattering angle 90 degrees.

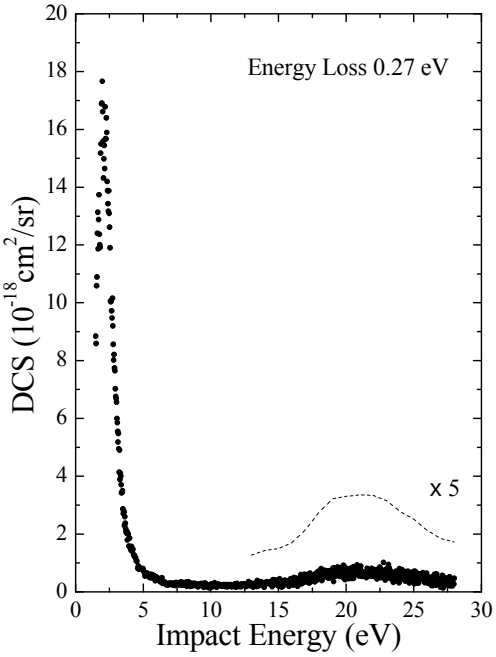

Figure C6.2. Vibrational excitation function of CO at the scattering angle of 90 degrees.

Table C6.1. Vibrational fundamental modes.

Vibrational mode	Energy (eV)	Species
CO str	0.270	σ^+

C7. OCS

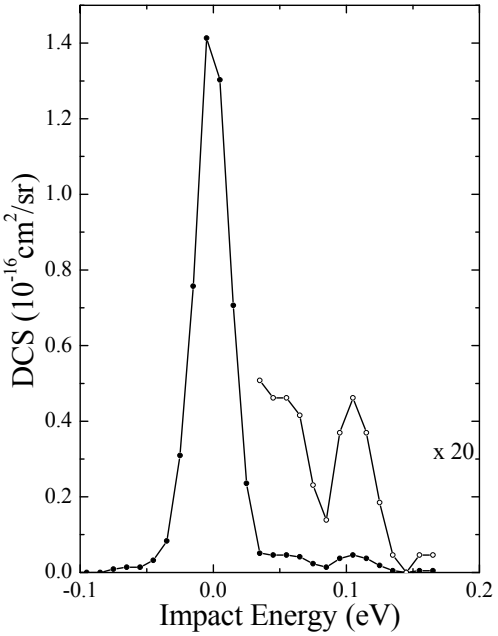

Figure C7.1. Energy loss spectrum of OCS at impact energy 3 eV for a scattering angle 90 degrees.

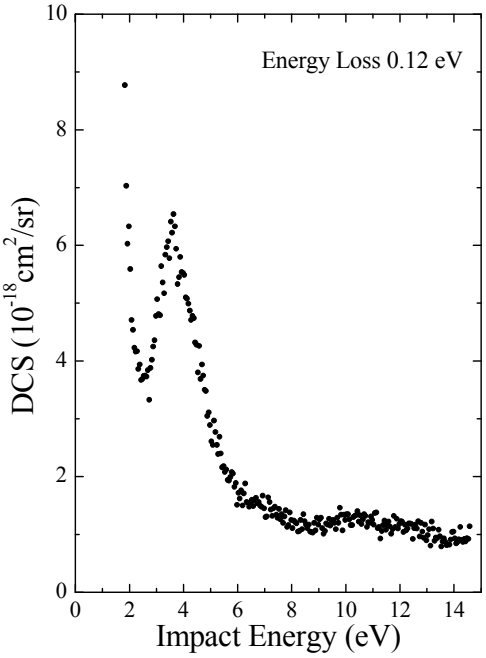

Figure C7.2. Vibrational excitation function of OCS at the scattering angle of 40 degrees.

Table C7.1. Vibrational fundamental modes.

Vibrational mode	Energy (eV)	Species
ν_1 (CO stretch)	0.256	σ^+
ν_2 (Bend)	0.064	π
ν_3 (CS stretch)	0.107	σ^+

C8. $\underline{CS_2}$

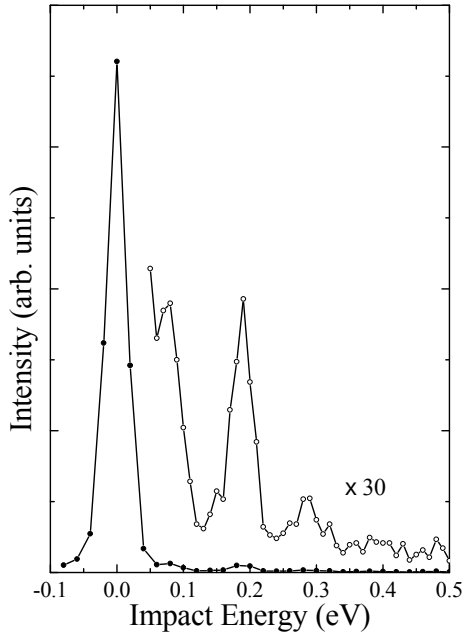

Figure C8.1. Energy loss spectrum of CS_2 at impact energy 2.8 eV for a scattering angle 30 degrees.

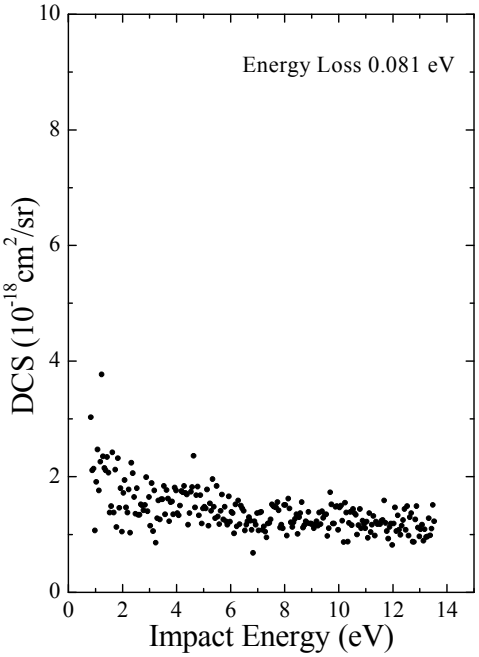

Figure C8.2. Vibrational excitation function of CS_2 at the scattering angle of 60 degrees.

Table C8.1. Vibrational fundamental modes.

Vibrational mode	Energy (eV)	Species
ν_1 (s-stretch)	0.082	σ_g^+
ν_2 (Bend)	0.049	π_u
ν_3 (a-stretch)	0.190	σ_u^+

C9. H_2O

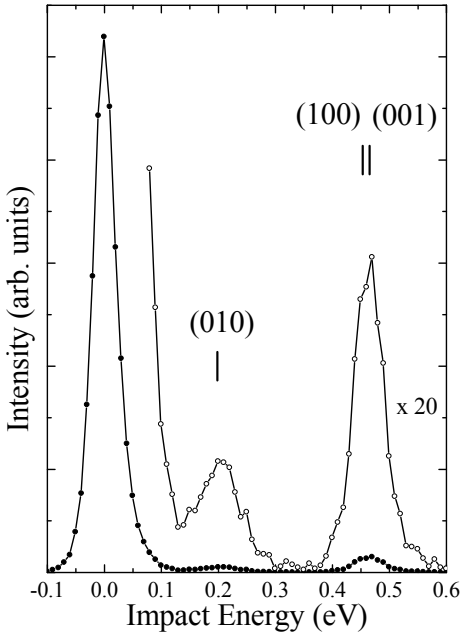

Figure C9.1. Energy loss spectrum of H_2O at impact energy 7.5 eV for a scattering angle 60 degrees.

Table C9.1. Vibrational fundamental modes.

Vibrational mode	Energy (eV)	Species
ν_1 (100), s-str	0.453	a_1
ν_2 (010), bend	0.198	a_1
ν_3 (001), a-str	0.465	b_1

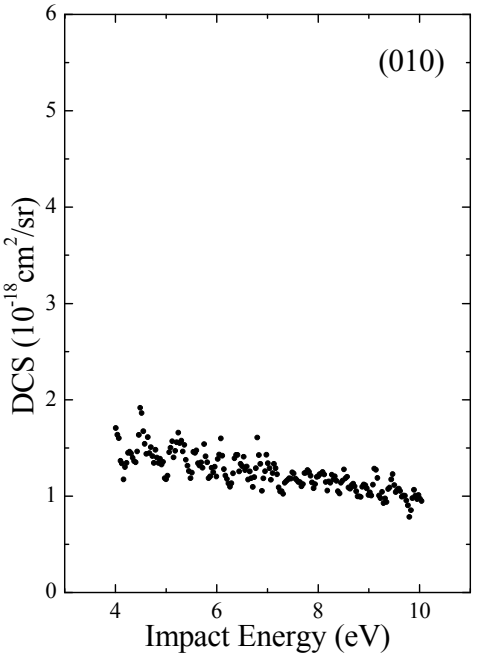

Figure C9.2. Vibrational excitation function of H_2O at the scattering angle of 60 degrees.

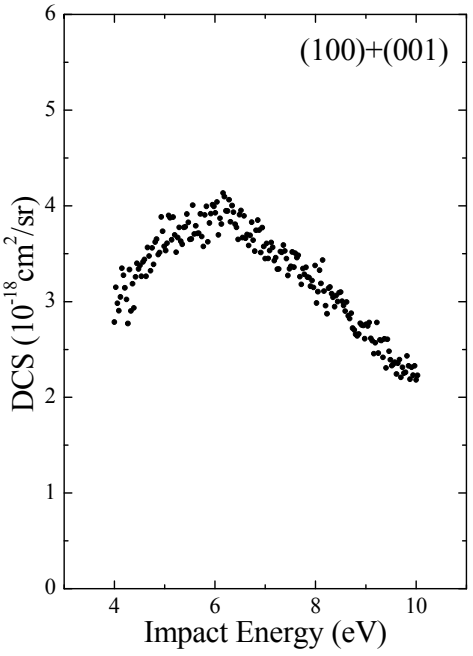

Figure C9.3. Vibrational excitation function of H_2O at the scattering angle of 60 degrees.

Reference:

C. Makochekanwa, R. Kajita, H. Kato, M. Kitajima, H. Cho, M. Kimura and H. Tanaka, *J. Chem. Phys.* **122**, 014314 (2005).

C10. H_2CO

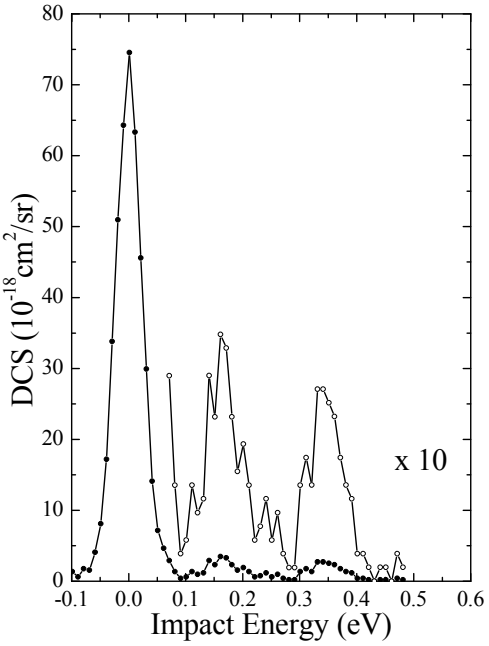

Figure C10.1. Energy loss spectrum of H_2CO at impact energy 7.5 eV for a scattering angle 90 degrees.

Table C10.1. Vibrational fundamental modes.

Vibrational mode	Energy (eV)	Species
ν_1 (CH_2 s-str)	0.345	a_1
ν_2 (CO str)	0.216	a_1
ν_3 (CH_2 scis)	0.186	a_1
ν_4 (CH_2 a-str)	0.352	b_1
ν_5 (CH_2 rock)	0.155	b_1
ν_6 (CH_2 wag)	0.145	b_2

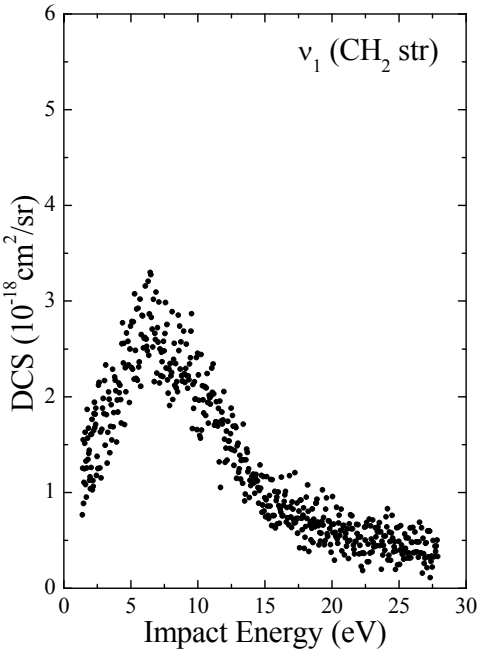

Figure C10.2. Vibrational excitation function of H_2CO at the scattering angle of 90 degrees.

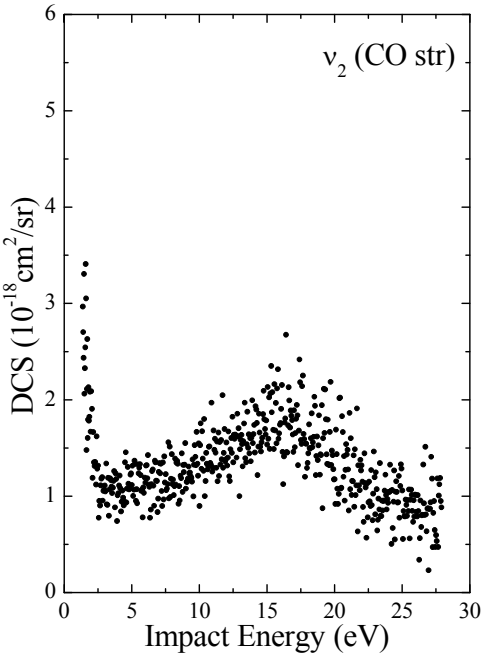

Figure C10.3. Vibrational excitation function of H_2CO at the scattering angle of 90 degrees.

Reference:

H. Kato, C. Makochekanwa, M. Hoshino, M. Kimura, H. Cho, T. Kume, A. Yamamoto, H. Tanaka, *Chem. Phys. Lett.* **425**, 1 (2006).

C11. $\underline{(CH_3)_2O}$

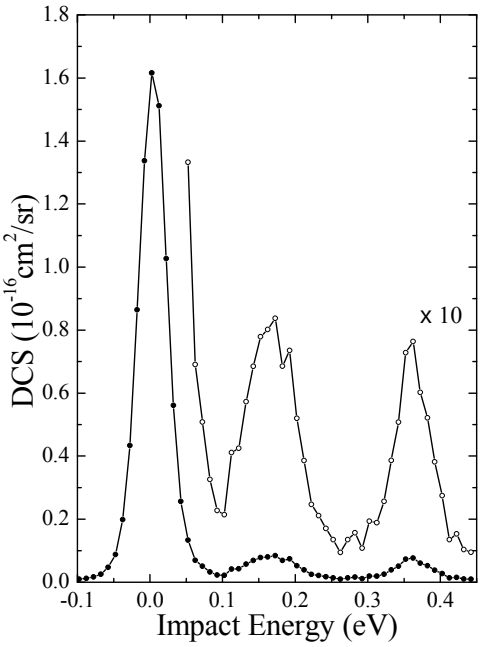

Figure C11.1. Energy loss spectrum of $(CH_3)_2O$ at impact energy 7.5 eV for a scattering angle 90 degrees.

Table C11.1. Vibrational fundamental modes.

Vibrational mode	Energy (eV)	Species
ν_1 (CH_3 d-str)	0.371	a_1
ν_2 (CH_3 s-str)	0.349	a_1
ν_3 (CH_3 d-deform)	0.182	a_1
ν_4 (CH_3 s-deform)	0.180	a_1
ν_5 (CH_3 rock)	0.154	a_1
ν_6 (CO s-str)	0.115	a_1
ν_7 (COC deform)	0.052	a_1
ν_8 (CH_3 d-str)	0.366	a_2
ν_9 (CH_3 d-deform)	0.182	a_2
ν_{10} (CH_3 rock)	0.143	a_2
ν_{11} (Torsion)	0.025	a_2
ν_{12} (CH_3 d-str)	0.371	b_1
ν_{13} (CH_3 s-str)	0.349	b_1
ν_{14} (CH_3 d-deform)	0.182	b_1
ν_{15} (CH_3 s-deform)	0.180	b_1
ν_{16} (CH_3 rock)	0.152	b_1
ν_{17} (CO a-str)	0.137	b_1
ν_{18} (CH_3 d-str)	0.363	b_2
ν_{19} (CH_3 d-deform)	0.182	b_2
ν_{20} (CH_3 rock)	0.146	b_2
ν_{21} (Torsion)	0.030	b_2

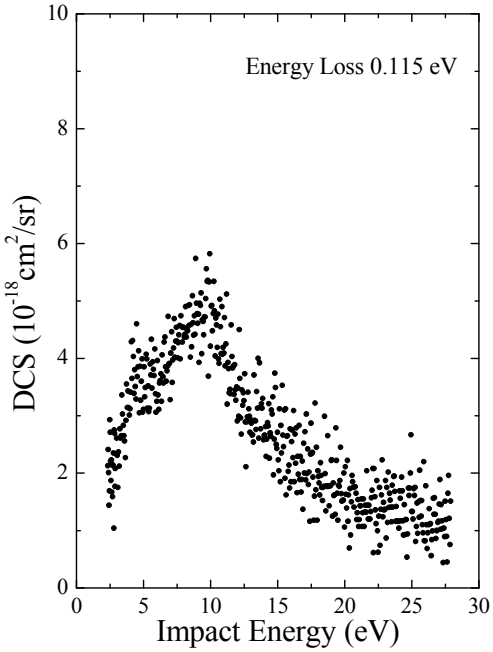

Figure C11.2. Vibrational excitation function of $(CH_3)_2O$ at the scattering angle of 90 degrees.

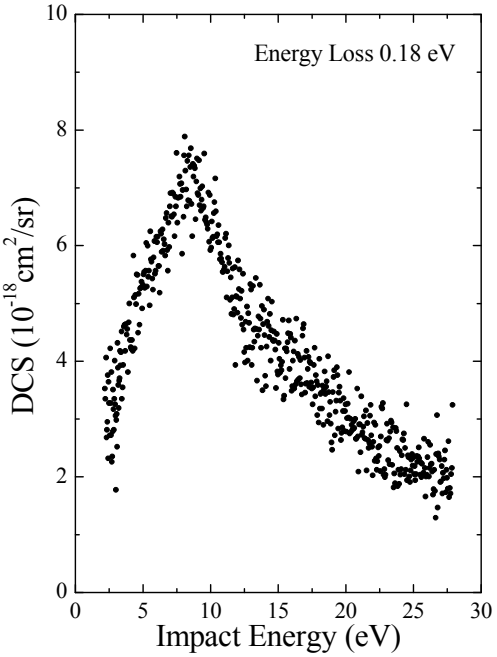

Figure C11.3. Vibrational excitation function of $(CH_3)_2O$ at the scattering angle of 90 degrees.

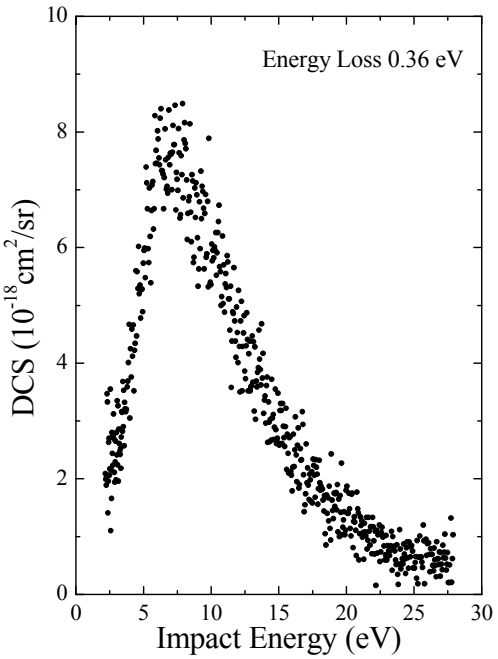

Figure C11.4. Vibrational excitation function of $(CH_3)_2O$ at the scattering angle of 90 degrees.

C12. $(CH_3)_2CO$

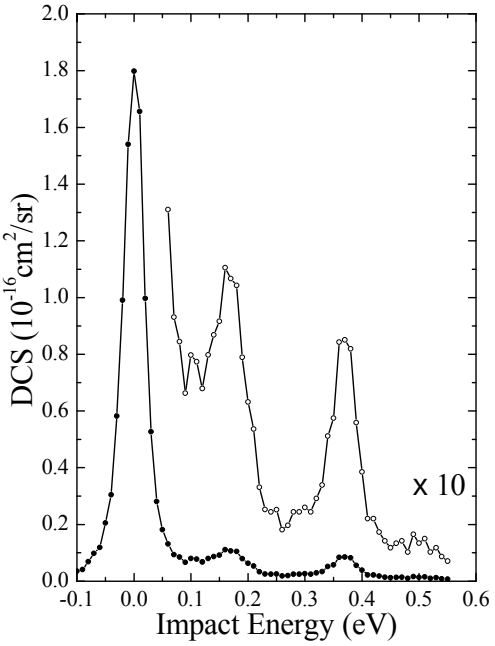

Figure C12.1. Energy loss spectrum of $(CH_3)_2CO$ at impact energy 7.5 eV for a scattering angle 90 degrees.

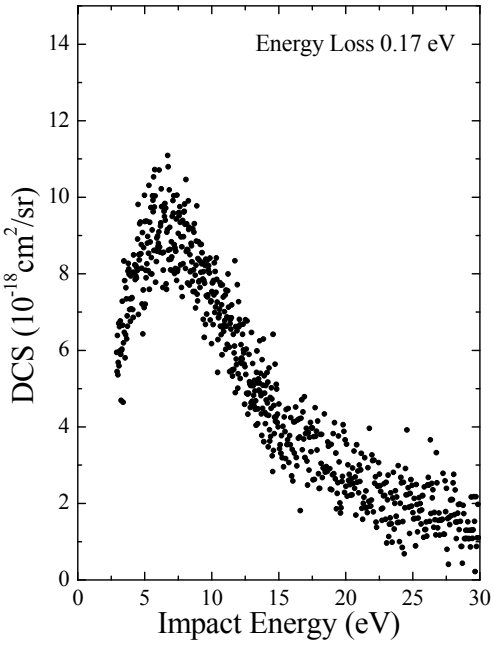

Figure C12.2. Vibrational excitation function of $(CH_3)_2CO$ at the scattering angle of 90 degrees.

Table C12.1. Vibrational fundamental modes.

Vibrational mode	Energy (eV)	Species
ν_1 (CH_3 d-str)	0.374	a_1
ν_2 (CH_3 s-str)	0.364	a_1
ν_3 (CO str)	0.215	a_1
ν_4 (CH_3 d-deform)	0.178	a_1
ν_5 (CH_3 s-deform)	0.169	a_1
ν_6 (CH_3 rock)	0.132	a_1
ν_7 (CC str)	0.096	a_1
ν_8 (CCC deform)	0.048	a_1
ν_9 (CH_3 d-str)	0.367	a_2
ν_{10} (CH_3 d-deform)	0.177	a_2
ν_{11} (CH_3 rock)	0.109	a_2
ν_{12} (Torsion)	0.013	a_2
ν_{13} (CH_3 d-str)	0.374	b_1
ν_{14} (CH_3 s-str)	0.364	b_1
ν_{15} (CH_3 d-deform)	0.175	b_1
ν_{16} (CH_3 s-deform)	0.169	b_1
ν_{17} (CC str)	0.151	b_1
ν_{18} (CH_3 rock)	0.110	b_1
ν_{19} (CO ip-bend)	0.066	b_1
ν_{20} (CH_3 d-str)	0.368	b_2
ν_{21} (CH_3 d-deform)	0.180	b_2
ν_{22} (CH_3 rock)	0.135	b_2
ν_{23} (CO op-bend)	0.060	b_2
ν_{24} (Torsion)	0.014	b_2

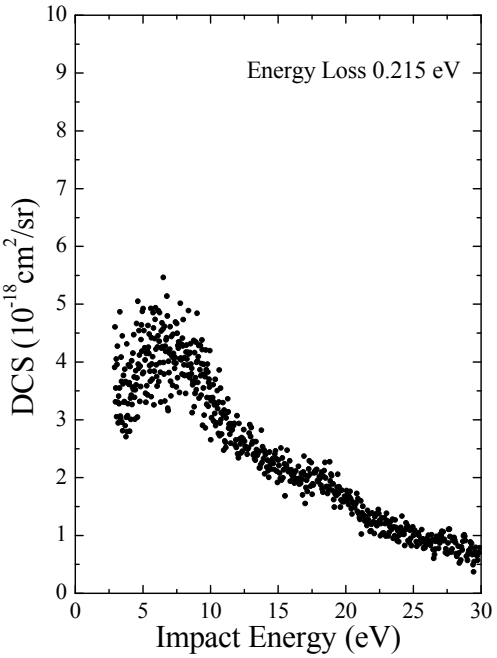

Figure C12.3. Vibrational excitation function of $(CH_3)_2CO$ at the scattering angle of 90 degrees.

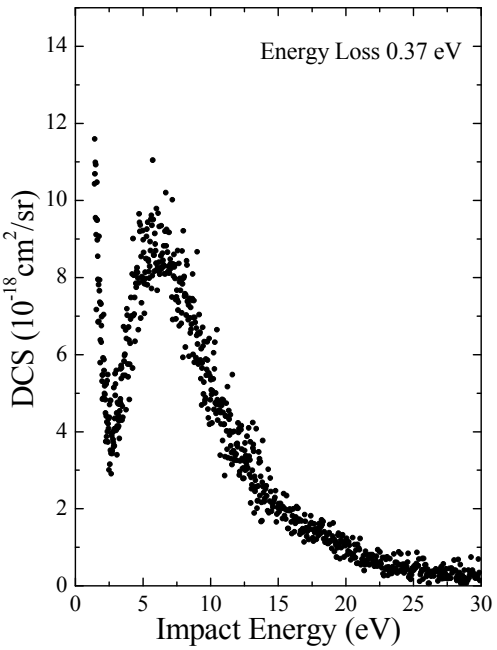

Figure C12.4. Vibrational excitation function of $(CH_3)_2CO$ at the scattering angle of 90 degrees.

C13. C_6H_6

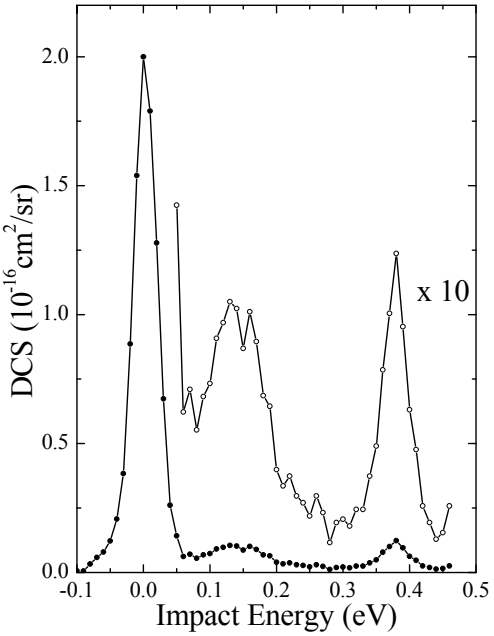

Figure C13.1. Energy loss spectrum of C_6H_6 at impact energy 7.5 eV for a scattering angle 90 degrees.

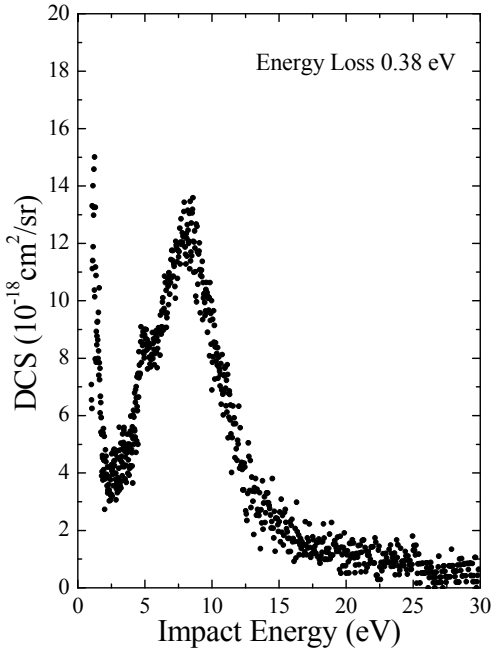

Figure C13.2. Vibrational excitation function of C_6H_6 at the scattering angle of 90 degrees.

Table C13.1. Vibrational fundamental modes.

Vibrational mode	Energy (eV)	Species
ν_1 (CH str)	0.380	a_{1g}
ν_2 (Ring str)	0.123	a_{1g}
ν_3 (CH bend)	0.164	a_{2g}
ν_4 (CH bend)	0.083	a_{2u}
ν_5 (CH str)	0.380	b_{1u}
ν_6 (Ring deform)	0.125	b_{1u}
ν_7 (CH bend)	0.123	b_{2g}
ν_8 (Ring deform)	0.087	b_{2g}
ν_9 (Ring str)	0.162	b_{2u}
ν_{10} (CH bend)	0.143	b_{2u}
ν_{11} (CH bend)	0.105	e_{1g}
ν_{12} (CH str)	0.380	e_{1u}
ν_{13} (Ring str + deform)	0.184	e_{1u}
ν_{14} (CH bend)	0.129	e_{1u}
ν_{15} (CH str)	0.378	e_{2g}
ν_{16} (Ring str)	0.198	e_{2g}
ν_{17} (CH bend)	0.146	e_{2g}
ν_{18} (Ring deform)	0.075	e_{2g}
ν_{19} (CH bend)	0.121	e_{2u}
ν_{20} (Ring deform)	0.051	e_{2u}

C14. $C_6H_5CH_3$

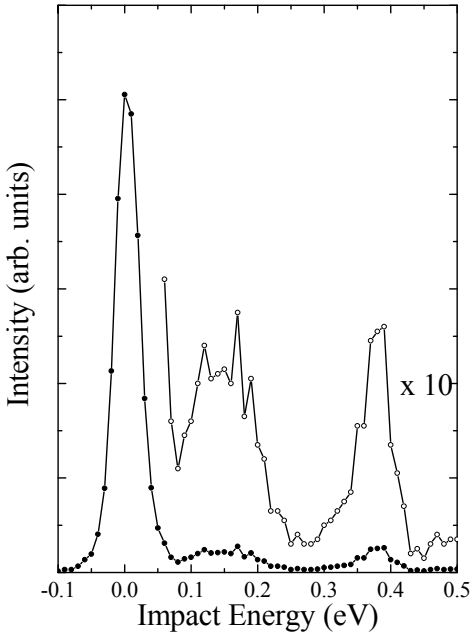

Figure C14.1. Energy loss spectrum of $C_6H_5CH_3$ at impact energy 7.5 eV for a scattering angle 90 degrees.

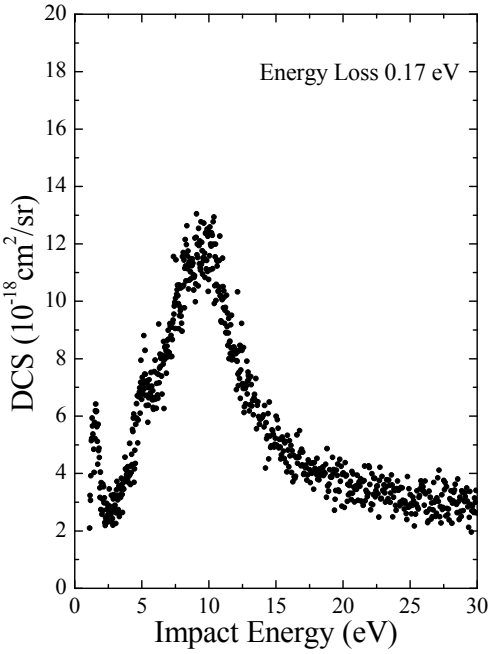

Figure C14.2. Vibrational excitation function of $C_6H_5CH_3$ at the scattering angle of 90 degrees.

Table C14.1. Vibrational fundamental modes. (*NIST* Data Theory)

Vibrational mode	Energy (eV)	Species
ν_1	0.382	a'
ν_2	0.379	a'
ν_3	0.378	a'
ν_4	0.369	a'
ν_5	0.362	a'
ν_6	0.198	a'
ν_7	0.184	a'
ν_8	0.181	a'
ν_9	0.172	a'
ν_{10}	0.148	a'
ν_{11}	0.145	a'
ν_{12}	0.128	a'
ν_{13}	0.126	a'
ν_{14}	0.121	a'
ν_{15}	0.118	a'
ν_{16}	0.108	a'
ν_{17}	0.095	a'
ν_{18}	0.089	a'
ν_{19}	0.085	a'
ν_{20}	0.063	a'
ν_{21}	0.057	a'
ν_{22}	0.025	a'
ν_{23}	0.380	a"
ν_{24}	0.378	a"
ν_{25}	0.372	a"
ν_{26}	0.196	a"
ν_{27}	0.182	a"
ν_{28}	0.178	a"
ν_{29}	0.163	a"
ν_{30}	0.161	a"
ν_{31}	0.142	a"
ν_{32}	0.134	a"
ν_{33}	0.121	a"
ν_{34}	0.115	a"
ν_{35}	0.102	a"
ν_{36}	0.076	a"
ν_{37}	0.050	a"
ν_{38}	0.041	a"
ν_{39}	0.004	a"

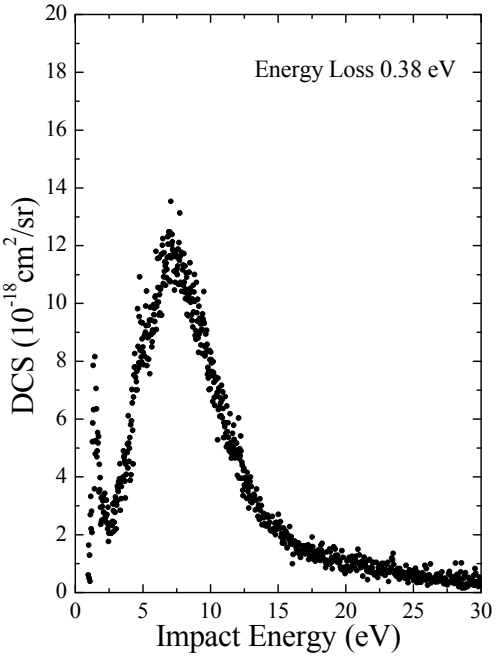

Figure C14.3. Vibrational excitation function of $C_6H_5CH_3$ at the scattering angle of 90 degrees.

Reference:

H. Kato, C. Makochekanwa, Y. Shiroyama, M. Hoshino, N. Shinohara, O. Sueoka, M. Kimura and H. Tanaka, *Phys. Rev. A.* **75**, 062705 (2007).

C15. $C_6H_5CF_3$

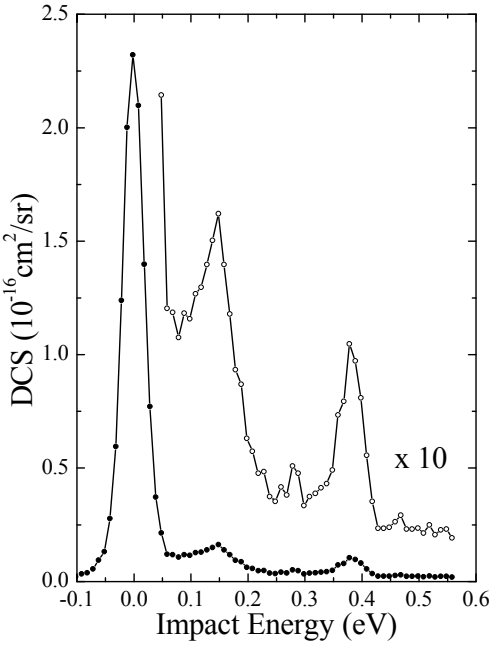

Figure C15.1. Energy loss spectrum of $C_6H_5CF_3$ at impact energy 7.5 eV for a scattering angle 90 degrees.

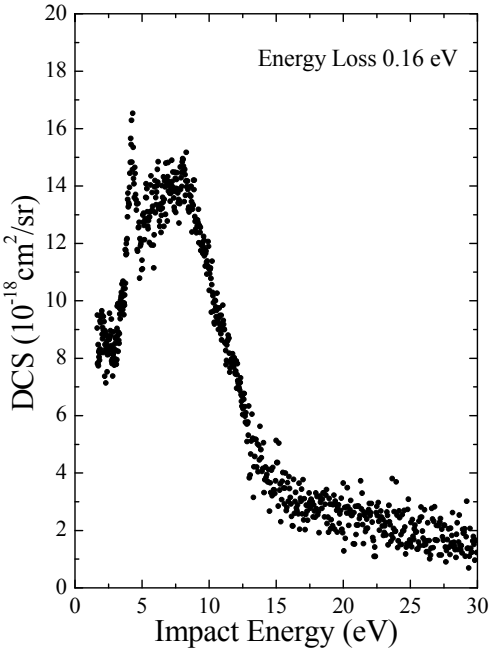

Figure C15.2. Vibrational excitation function of $C_6H_5CF_3$ at the scattering angle of 90 degrees.

Table C15.1. Vibrational fundamental modes.

Vibrational mode	Energy (eV)	Species
ring deform	0.042	a_1
ring breathing	0.095	a_1
C-CF_3 str	0.127	a_1
C-H bending	0.133	a_1
C-H bending	0.146	a_1
ring deform	0.181	a_1
ring deform	0.200	a_1
C-H str	0.384	a_1
C-H bending	0.112	b_1
C-H bending	0.153	b_1
ring deform	0.169	b_1
ring deform	0.181	b_1
ring deform	0.200	b_1
C-H str	0.384	b_1
ring deform	0.060	b_2
ring deform	0.086	b_2
C-H bending	0.095	b_2
C-H bending	0.114	b_2
CF_3 rock	0.039	
CF_3 rock	0.049	
a-CF_3 deform	0.074	
s-CF_3 deform	0.081	
a-CF_3 str	0.143	
s-CF_3 str	0.165	

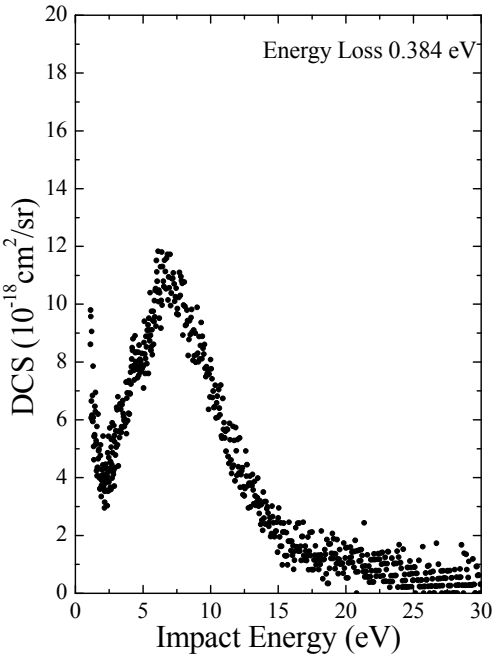

Figure C15.3. Vibrational excitation function of $C_6H_5CF_3$ at the scattering angle of 90 degrees.

C16. 1.1-$C_2H_2F_2$

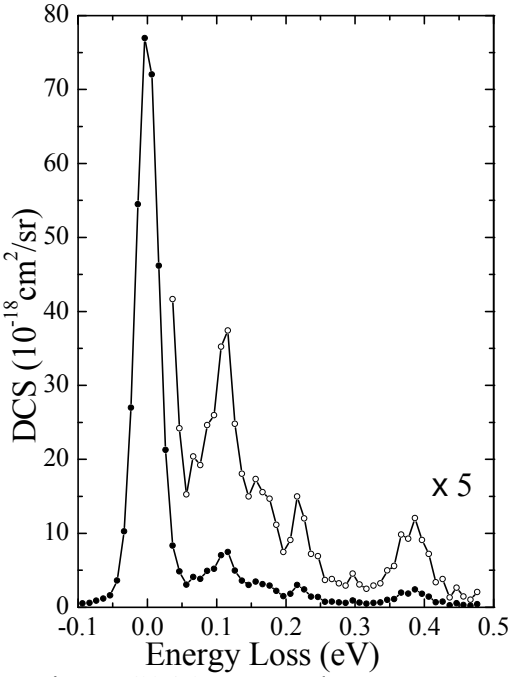

Figure C16.1. Energy loss spectrum of 1.1-$C_2H_2F_2$ at impact energy 7.5 eV for a scattering angle 90 degrees.

Table C16.1. Vibrational fundamental modes.

Vibrational mode	Energy (eV)	Species
ν_1 (CH_2 s-str)	0.381	a_1
ν_2 (CC str)	0.214	a_1
ν_3 (CH_2 scis)	0.169	a_1
ν_4 (CF_2 s-str)	0.115	a_1
ν_5 (CF_2 scis)	0.068	a_1
ν_6 (Torsion)	0.089	a_2
ν_7 (CH_2 a-str)	0.100	b_1
ν_8 (CH_2 rock)	0.076	b_1
ν_9 (CF_2 a-str)	0.391	b_2
ν_{10} (CF_2 rock)	0.161	b_2
ν_{11} (CH_2 wag)	0.118	b_2
ν_{12} (CF_2 wag)	0.054	b_2

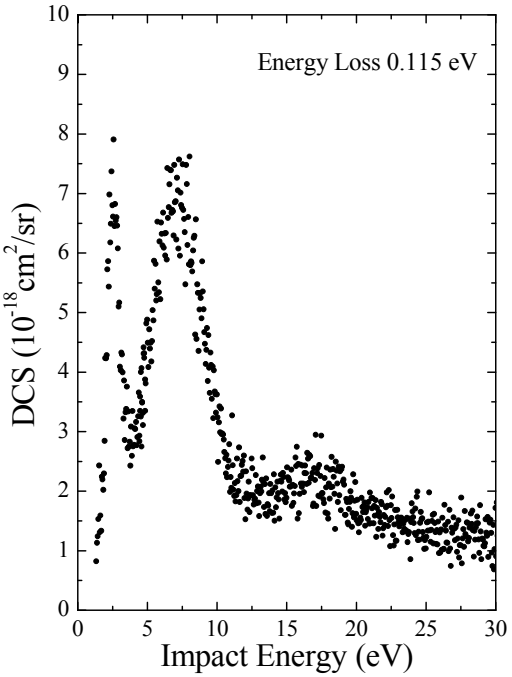

Figure C16.2. Vibrational excitation function of 1.1-$C_2H_2F_2$ at the scattering angle of 90 degrees.

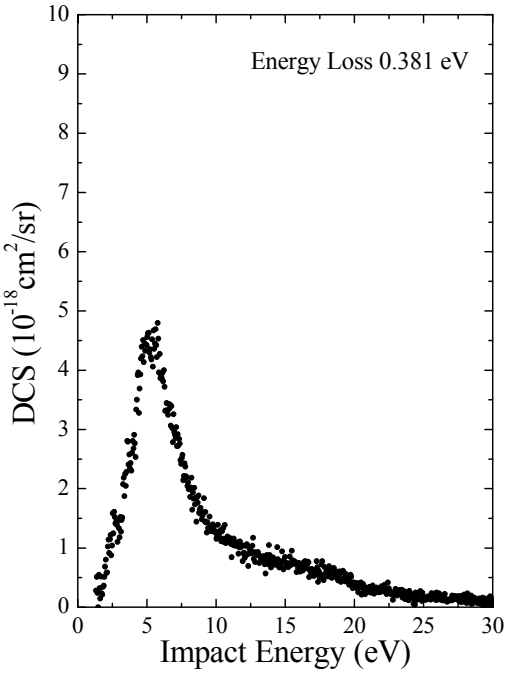

Figure C16.3. Vibrational excitation function of 1.1-$C_2H_2F_2$ at the scattering angle of 90 degrees.

Reference:

C. Makochekanwa, H. Kato, M. Hoshino, M. H. F. Bettega, M. A. P. Lima, O. Sueoka, H. Tanaka, *J. Chem. Phys.* **126**, 164309 (2007).

4. Concluding remarks

Excellent reviews on resonances in electron scattering have been available for atoms and molecules in such examples as the *Rev. Mod. Phys.*(Schulz), as well as in the *J. Electron Spectrosc. Relat. Phenom.* (Allan), as cited above. Although the concept of a resonance process was described clearly and discussed fully, its effect on the vibrational cross sections has ensured that the modelling data needs turned out to be demanding from the view point of applications in discharge plasmas, in general. It has for instance been well recognized that vibrational excitation plays an important role in the science of the gas laser. One of the most efficient laser systems designed to date, the N_2-CO_2 laser, relies on vibrational transitions for laser action. In the N_2-CO_2 system the large vibrational cross section, resulting from a $^2\Pi g$ shape resonance near 2.3 eV in N_2, causes the electron distribution function to be sharply cut off. This results in an efficient population of vibrational levels in N_2, with subsequent transfer to the upper laser state of CO_2 (the asymmetric stretch mode). In this report, the broad peaks in the vibrational cross section caused by shape resonances were summarized for 35 molecules categorized into three groups of A) Fusion Plasma-related Gases, B) Processing Plasma-related Gases, and C) Environmental Issues-related Gases. From this report, it is clear that resonances occurring in electron impact often enhance inelastic cross sections by an order of magnitude and sometimes the energy dependence of these cross sections exhibits oscillatory structure or isolated peaks. The position of the resonance is, at a glance, found in the relevant Figures for each molecule, in which the cross section is shown on an absolute scale.

Reaction mechanisms in discharge plasmas can be classified into three stages of temporal development, starting with plasma initiation and ending with product formation, which may be designated as “physical”, “physicochemical”, and “chemical”. The physical stage consists of excitation and ionization of atoms and molecules of the material gas by electron impact. The physicochemical stage consists of rapid reactions of highly active species, such as slow electrons, positive or negative ions, excited atoms, and radicals resulting from molecular dissociation, with atoms or molecules of the material gas mostly in their ground states. The chemical stage consists of thermal reactions of the products of the physicochemical stage, with atoms and molecules of the material gas. In each process, the secondary electrons play the most important role in sustaining the plasma condition of detail balance with the positive ions, which includes also energy-degradation through inelastic collision processes with molecules.

We thus hope that this report might serve as a data resource for trying to quantitatively understand the contribution of vibrational-excitation in practical plasma structures.

Acknowledgements

This work is performed under the IAEA Coordinated Research Program on Atomic and Molecular Data for Plasma Modeling for seven of the authors (M.H., C.M., S.J.B., M.J.B., H.C., M.K., and H.T.), and supported, in part, by the Ministry of Education, Science, Technology, Sport and Culture, Japan (M.H. an H.T.), the Core University Program of the Japan Society for the Promotion of Science (H.C. and H.T.), and the National Institute of Fusion Science, Japan (D.K.,I.M.,T.K., and H.T.). Two of the authors (S.J.B and M.J.B) acknowledge also the Australian Research Council for the ARC Linkage International Program between Australia, Korea and Japan.